GEAR TECHNOLOGY

The Journal of Gear Manufacturing

MAY/JUNE 1988

Curvilinear Cylindrical Gears

Tooth Root Stresses of Spiral Bevel Gears

Computer-Aided Design — Stress Analysis of an Internal Spur Gear

Helical Gear Mathematics

GEAR TECHNOLOGY

The Journal of Gear Manufacturing

RANDALL PUBLISHING
1401 Lunt Avenue
P.O. Box 1426
Elk Grove, IL 60007
(312) 437-6604

COVER

"South Pointing Chariot." An example of "an ancient Chinese vehicle with a wooden figure always pointing to the south," similar figures are found in archeological digs in China. Their exact purpose is open to debate, but one common theory is that they were used as a kind of compass on long wilderness and desert journeys. Although they are not visible on this model, curvilinear gears are the likely driving mechanism on the original devices. The figure on our cover is a contemporary working model using a system of differential gears. It was produced by Mr. Don Frantz of Burbank, CA.

CONTENTS — PAGE NO.

FEATURES

DEPARTMENTS

May/June 1988 — Vol. 5, No. 3

GEAR TECHNOLOGY, The Journal of Gear Manufacturing (ISSN 0743-6858) is published bimonthly by Randall Publishing Co., Inc., 1425 Lunt Avenue, P. O. Box 1426, Elk Grove Village, IL 60007. GEAR TECHNOLOGY, The Journal of Gear Manufacturing is distributed free of charge to qualified individuals and firms in the gear manufacturing industry. Subscription rates for non-qualified individuals and firms are: $35.00 in the United States, $55.00 for foreign countries. Second-Class postage paid at Arlington Heights, IL and at additional mailing office.
Postmaster: Send address changes to GEAR TECHNOLOGY, The Journal of Gear Manufacturing, 1425 Lunt Avenue, P. O. Box 1426, Elk Grove Village, IL 60007.

MANUSCRIPTS: We are requesting technical papers with an educational emphasis for anyone having anything to do with the design, manufacture, testing or processing of gears. Subjects sought are solutions to specific problems, explanations of new technology, techniques, designs, processes, and alternative manufacturing methods. These can range from the "How to . . ." of gear cutting (BACK TO BASICS) to the most advanced technology. All manuscripts submitted will be carefully considered. However, the Publisher assumes no responsibility for the safety or return of manuscripts. Manuscripts must be accompanied by a self-addressed, self-stamped envelope, and be sent to GEAR TECHNOLOGY, The Journal of Gear Manufacturing, P.O. Box 1426, Elk Grove, IL 60007, (312) 437-6604.

EDITORIAL

CRISIS AND CHALLENGE IN AMERICAN EDUCATION

"We have met the enemy and he is us," says Pogo, the cartoon character. The enemy is the crisis in our educational system, and "crisis" is the only term that accurately describes the situation. It is every bit as serious, if not more so, than the crisis that followed the Soviet launching of Sputnik in 1957 — and for many of the same reasons. Our failing public education system threatens our position in the global political and business arenas; and this time, it's not just the Soviets or the Japanese who need to be taken seriously as competitors. Every country in the world that graduates better prepared students than we do — and there are a great many of them — has us at a competitive disadvantage.

My personal concern, and, frankly, sense of frustration have been raised by a number of items which have crossed my desk in the last few months. Late last year, Secretary of Education, William Bennett, recommended a basic core curriculum for American high schools emphasizing writing, reading, language, history, science, math, art, music and physical education; and then he pointed out that only 15% of the high schools in this country now offer such a progam to their students. At the same time, according to *Business Week* magazine, federal spending for education has dropped 17%. In my own state, Illinois, a school pioneering in math and science for gifted students is in danger of closing because of lack of funds, and both the Illinois State Chamber of Commerce and the Illinois Manufacturers Association oppose any tax increases for education — out of fear that higher taxes will cause businesses to move elsewhere. It is disheartening to realize that neither government officials nor businesspeople seem to see the connection between poor education and a poor quality work force.

While your child or mine may not be victims of this crisis, all too many American children are barely literate after twelve years in our school system. Far too many young adults cannot read and write well enough to fill out a job application, and they cannot do math well enough to make change if the electronic cash register fails. They don't know an atom from an aardvark, much less have any ideas about or familiarity with "softer" subjects like art, literature or any music written before 1980. What is worse, they have been so turned off by their educational experience that they have no interest in any kind of formalized learning. The system as it works now doesn't provide basics for the average student, sufficient special help for the culturally and economically disadvantaged or academic challenge for the gifted.

Of course, not every school is a failure. Not every child is lost. We have some marvelous school systems that provide for the needs of most of their students and turn out fully prepared graduates. Unfortunately, there are not

nearly enough of such systems. Too many lose students to boredom, indifference or simple incompetence.

We can already see some of the results of this neglect. According to a study by the U.S. Science Foundation, which compared the scientific education of students from several countries, American students ranked below the middle of the scale. U.S. high school seniors were near the bottom. Last year, 55.4% of the engineering doctoral degrees granted in the U.S. went to overseas students. At Penn State, the figure was 74%.

The problem isn't that we're training too many foreign students, but that we're not training enough of our own. While our best universities are still providing advanced education that is the envy of the world, many of our own citizens are not well enough prepared to take advantage of it. Corporate recruiters for some of the country's leading technological firms complain that they cannot find a single, qualified American to hire.

Easy answers to this problem don't exist. Wringing our hands, pointing fingers of blame or establishing quotas to limit the number of foreign students training in the U.S. are not really helpful solutions. Neither is simply throwing money at the problem.

We must seriously reassess the place that education holds in our own minds. Do we really care about excellence in education, and are we willing to demand it of our own children? Since the improvement of the system starts at home, will we insist that the t.v. be turned off and the homework done? When the option is offered, are we willing to insist our children take a challenging course instead of one that is "fun", and then are we willing to take the time to work with them and their teachers, or go to school meetings and conferences? To a large degree, our children will take their cues about the importance of their education from us.

More than this sacrifice of time and effort, we are going to have to be prepared to sacrifice some money, and, perhaps more painful, some of our most cherished presuppositions. This country has some enormous economic and fiscal problems to solve, and the educational crisis is part of this larger picture. We are facing some tough choices and some favorite "untouchable" spending programs may have to be touched after all. Everyone's campaign promises to the contrary, we all may have to pay higher taxes.

At the same time, we have to give up the idea that dealing with the educational crisis — either fiscally or philosophically — is the exclusive responsibility of the state or federal government. Education has always been a local issue, a place where individual citizens were deeply involved. People like us are the ones who run for the school board and the PTA, make the phone calls and write the letters that motivate change. A hassle perhaps, but historically, that is the way the job gets done.

Businesses can respond directly to the crisis in education too. An entrepreneur and philanthropist in New York adopted an entire sixth grade class in the South Bronx. He promised a complete scholarship to each child that completed high school with good grades. Better than three-fourths of them accepted his offer. Few of us have the wealth to do something on that scale, but we can involve ourselves in creative ways like internship programs, joint ventures and corporate or trade association scholarships. This is not the time to reject plans just because they are innovative or non-traditional.

Certainly such ventures take time and money, but we either become more involved in the business of improving our schools now, or we pay later when we have to implement programs to retrain workers to tasks they should have learned in school in the first place.

We need a change in our national attitude and resolution, just as we did at the beginning of the space program. We must tell our elected officials that we are serious about improving the educational system and are willing to make the necessary sacrifices to do it. We can't expect politicians to commit political suicide. If we routinely respond to the candidate who offers us the easy, short term solution at the price of a mortgaged future farther down the road, then we cannot be surprised if that is what we get.

Secretary of Education William Bennett demands that we "raise the expectations" for our children, demanding the best from them. At the same time, we should "raise the expectations" for our politicians and ourselves as well. We can demand more than the cheap, easy, popular or facile solution to our problems, and by demanding it, we will eventually get it. A democratic country gets the government it deserves — and the government it asks for.

This is a presidential election year. It is the perfect opportunity to get the message across to those we are sending to Washington, to our state capitals, and to our local government buildings. The message is that we need a better educational system and that we are willing to work, sacrifice and support officials who will provide us with the necessary leadership to get the job done.

What is at stake here is nothing less than our children's and grandchildren's futures — futures conceivably populated with more and more under-educated people pushed out into society where they can function only minimally. The longer we wait, the higher the price becomes. If we don't give American children the best training possible, we deprive them of the tools necessary for their own welfare and for the welfare of the country as a whole.

The crisis in American education is real. It is as real a threat as any disease, invasion or high tech weapon. If we ignore it, it will go away — along with any opportunity for our country to maintain its standard of living and its position of leadership in the world.

Michael Goldstein, Editor/Publisher

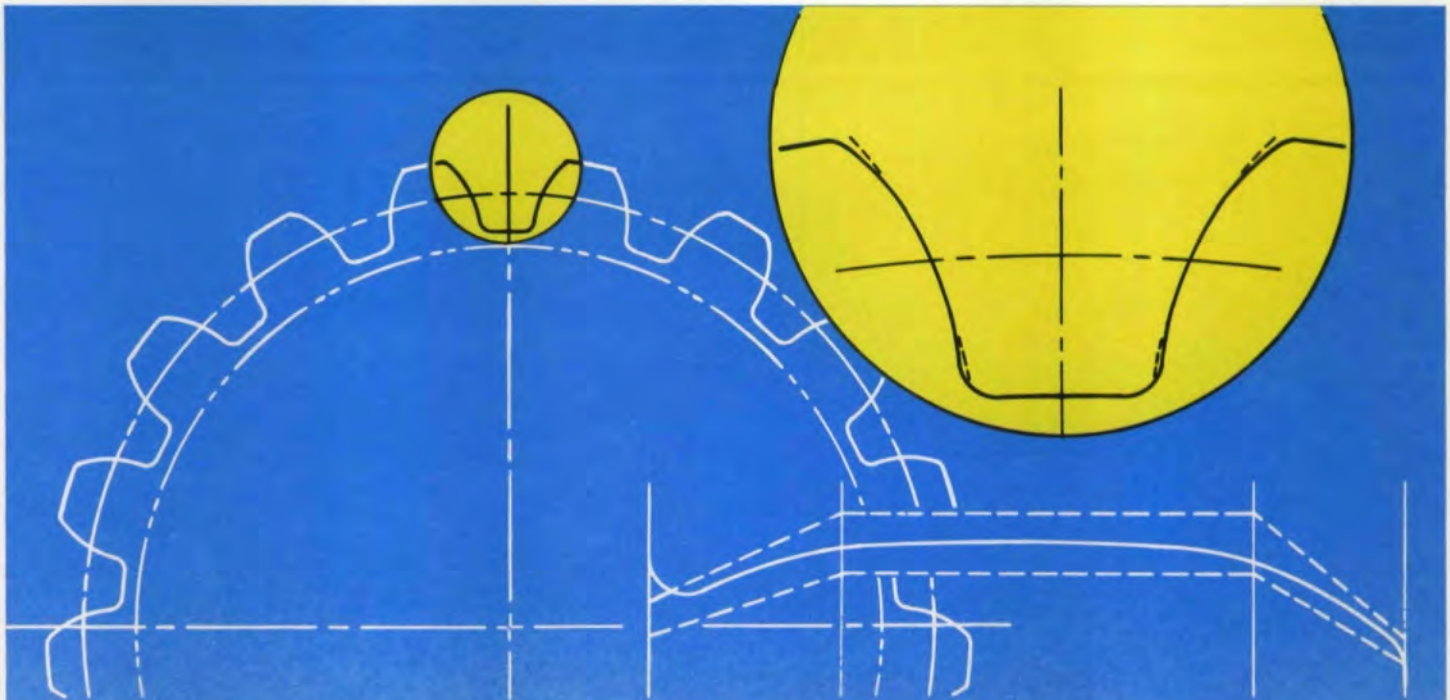

When you need critical accuracy time, after time, after time...

You need Normac's Formaster CNC Grinding Wheel Profiler

The Formaster gives you inspection guage accuracy

Normac guarantees an accuracy of ± .0001" (.002 mm) from programed dimensions and provides less than .0001" (.002 mm) positioning error throughout total slide travel.

Easily adaptable to meet your need.

The Formaster is designed to mount easily on nearly any type of grinding machine. It is compact and lightweight and just a mounting bracket and only minor machine modifications are required for installation on most grinders. Installation usually takes one day or less.

The unique features of Normac's Formaster.

- The unit is totally sealed and air-purged for trouble-free operation and protection from coolant contamination.
- Double nut pre-loaded roller screws transmit servo motor to slide movement.
- Optional rotary diamond dressing wheel attachment provides greater accuracy and eliminates error caused by single point diamond wear.

Formaster users have reported increased production and greater accuracy.

- Increase in wheel life of up to 8-10 times longer than with other units.
- Production increases up to 20% in the first two weeks of use.
- Set-up-time is reduced to 80% of what it used to be with improved surface integrity of the parts.
- Eliminates need for skilled operators as the unit is automatic. Unit can be retro-fit for use with automatic infeed.

Now Normac offers you software for the Formaster for automatic program generation.

Normac has developed optional software that runs on a personal computer in a question and answer format. It allows the user to enter part print specifications (including root and profile modifications) in standard gear nomenclature. The program outputs N.C. code loaded into the Formaster control for wheel profiling, and also detailed printouts suitable for gear profile analysis. This software contains logic for all types of root zone grinding, true involute and exponential flank modifications as well as "Proudness" of the entire profile as indicated in the K-diagram above.

Let us show you what the Formaster can do for your grinding operations

If you would like, we can arrange a demonstration of the Formaster for you. Call or write us today.

NORMAC, INC.

P.O. Box 69
Arden, N.C. 28704
(704) 684-1002

P.O. Box 207
Northville, MI 48167
(313) 349-2644

CIRCLE A-19 ON READER REPLY CARD

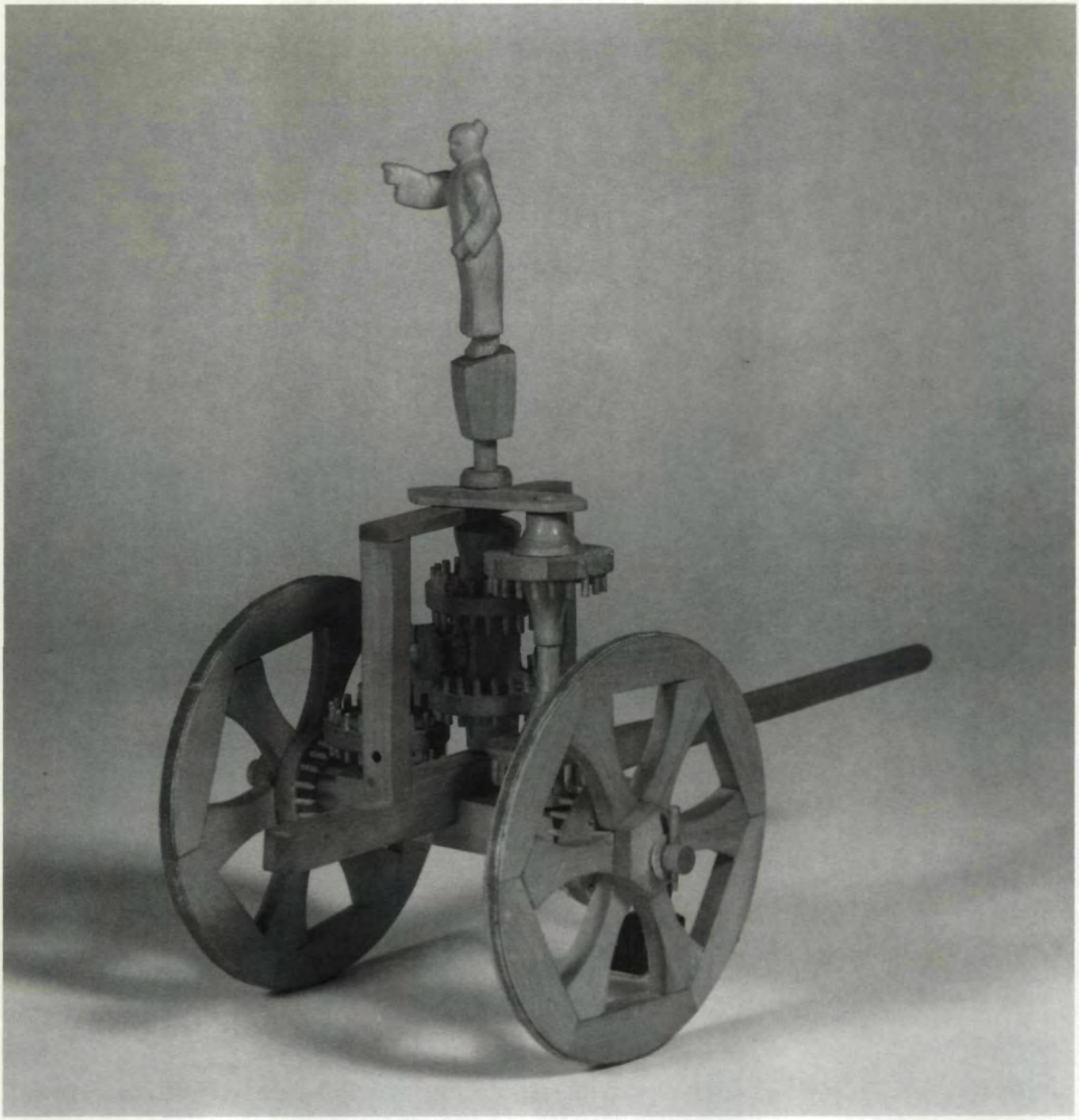

PHOTO COURTESY OF SMITHSONIAN INSTITUTION

Curvilinear Cylindrical Gears

Liu Shue-Tseng,
Shanghai Metallurgical Machinery Factory
Shanghai, People's Republic of China

(Photo on left) Wooden model of "South Pointing Chariot". Although the curvilinear gear is not visible on this model, such gears were used in the manufacture of these devices, which may have served as compasses in ancient times.

The curved tooth cylindrical gear is one of ancient design. Samples which date from the period of the Warring State (475-221 BC) have been excavated from archeological sites in China. One such sample is now on display in the Xi'an Clay Figures of Warriors and Horses Exhibition Hall. This example is about 3/4" in diameter and made of bronze. It was used in the famous model, "Ancient Chinese Vehicle With a Wooden Figure Always Pointing to the South." Although this early gear is handmade and somewhat crude, it is a viable model.

Chinese technologists have been interested in this ancient design, and, after overcoming some technical difficulties, we have successfully designed the special machine tools and manufacturing processes necessary to bring the curvilinear cylindral gear into practical production. The first marketable applications appeared in 1980. Photographs of some of these gears are shown in Fig. 1.

Fig. 1 – Some samples of curvilinear tooth gears.

Basic Curvilinear Cylindrical Gear Manufacture

Gear manufacturers and consumers are always searching for more compact or higher capacity gear sets. This design of gearing offers a way to achieve these characteristics. The basic manufacturing process is described below.

First imagine a tooth generating rack made of hard metal. The rack is kept stationery, and the form of its longitudinal tooth line is circular rather than the usual straight line. A plastically compliant gear blank is used and is run along the rack with a pure rolling motion, that is, with no slippage; thus, the blank is squeezed and extended to produce a circular toothed gear conjugate to the rack. (See Fig. 2.) If the tooth line of the rack were not circular, but of another form, the teeth produced on the blank would be of another curved form conjugate to that rack. All such curved tooth forms are called "curvilinear tooth cylindrical gears."

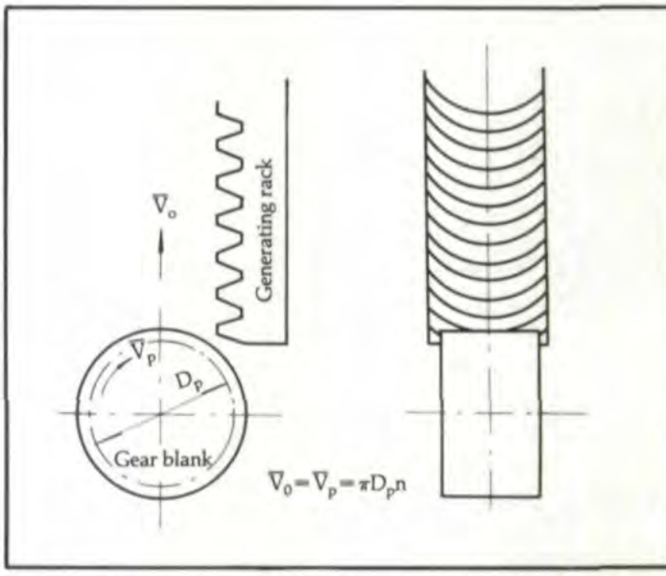

Fig. 2 – The generating principle of a curvilinear tooth cylindrical gear.

To produce such gears, the combined motion of the gear blank and rack must obey the following rule:

$$V_o = V_p = \pi D_p n \qquad (1)$$

where

- V_o – Linear translational velocity of the gear blank axis in meters per minute (m/min).
- V_p – Circular velocity of the blank on time pitch diameter in m/min.
- D_p – Pitch diameter in meters.
- π – Pi
- n – Rotational speed of the gear blank in rpms.

In practice we use a rotating face mill cutter to produce the gear teeth. The cutter spindle rotates on a fixed or stationary axis while the gear blank is rotated and translated across the turning cutter teeth according to Equation 1. By this rolling generating process the cutter produces one space on the gear. The blank is then indexed one tooth and the

AUTHOR:

LIU SHUE-TSENG *graduated from the Hong Chow University with Bachelor of Science in Mechanical Engineering. After his university work, he received additional training with National Agricultural Engineering Corporation. For the last 38 years he has been employed by the Shanghai Metallurgical Machinery Factory, working in foundry technology, as chief of the maintenance and design department and, since 1980, as senior chief engineer in charge of machine design and research work. Mr. Liu has been working on the curvilinear tooth cylindrical gear project since 1978.*

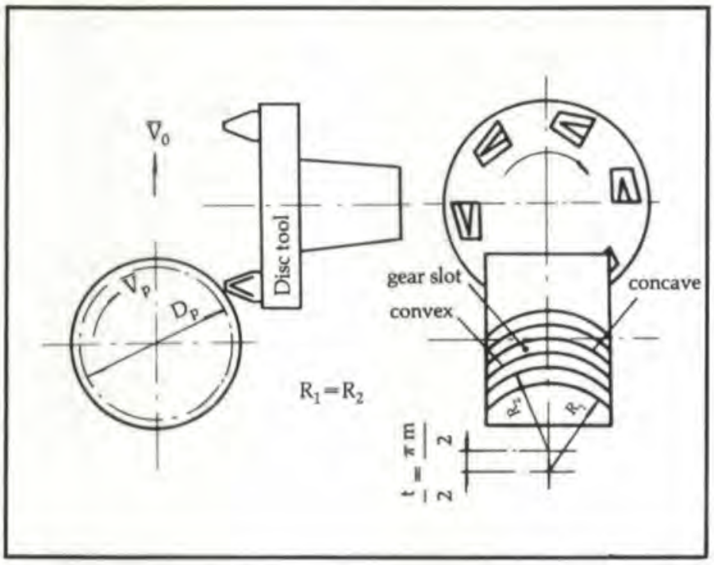

Fig. 3—Cutting a circular tooth gear with a disc tool.

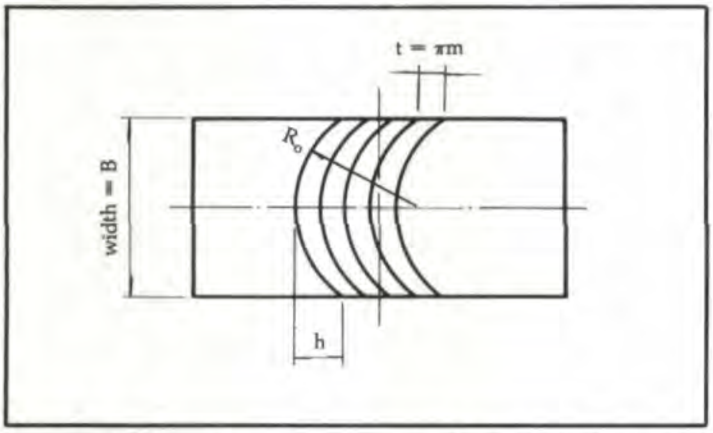

Fig. 4—The supplementary contact ratio of a circular tooth gear.

generating cycle repeated. This sequence is continued until all the spaces and teeth are formed. (See Fig. 3.)

Since the generating motions are relative, an alternate machine construction would have the gear axis fixed and the cutter translated past the gear blank. The results will be the same.

For ease in manufacturing, we made the profile on the cutter blades in the form of an isoceles trapezoid similar to the tool used in Acme thread turning. The generating action of this tool configuration develops a gear with an involute profile of pressure angle α in the central section and a hyperbolic evoluted profile in the off-center sections. But at any section across the gear face, its concave and convex flanks are conjugate, so any pair of gears can be properly meshed together.

Obviously, the radius of curvature on both flanks of the gear must be alike to achieve proper engagement. The radius of curvature on the outer form of the cutter teeth is larger than that on the inner form. So after the gear is formed by the first cutter, a second cutter is utilized to form the convex faces to the same radius as the concave flank. (See Fig. 3.)

We have now developed a continuous cutting process which provides greater manufacturing efficiency.

Strength Analysis of a Curvilinear Tooth

The Contact Ratio. According to the theory of mechanism, we know that the contact ratio of a spur gear is

$$E_o = E_1 + E_2 - E_A \tag{2}$$

$$E_o = \frac{\sqrt{(Z_1 + 2)^2 - (Z_1 \cos\alpha)^2}}{2\,\pi\cos\alpha} + \frac{\sqrt{(Z_2 + 2)^2 - (Z_2 \cos\alpha)^2}}{2\,\pi\cos\alpha} - (Z_1 + Z_2)\frac{\tan\alpha}{2\pi} \tag{2a}$$

where

Z_1 = number of teeth on the pinion
Z_2 = number of teeth on the gear.
α = the pressure angle.

A curvilinear gear tooth possesses the same contact ratio as a spur gear, plus a supplementary contact ratio due to face overlap. (See Fig. 4.)

The supplementary contact ratio of a curvilinear tooth gear is

$$E_S = \frac{h}{t} = \frac{h}{m\pi}$$

Where

t = Tooth pitch distance

m = Module of the gear

$h = R_o - \sqrt{R_o^2 - (\frac{B}{2})^2}$

R_o = Radius of tooth curvature

B = Gear face width

$\therefore$ the total contact ratio of a curvilinear tooth gear is

$$\Sigma E = E_o + E_S \tag{3}$$

Evidently, ΣE is greater than E_o. That means that a pair of curvilinear tooth gears has a greater number of gear teeth simultaneously in mesh; thus the force exerted on every individual tooth may be reduced materially.

For instance, if E_o of a spur gear equals 1.7, that means at a certain instant, only one tooth pair is meshing. But for a pair of curvilinear toothed gears, ΣE increased to 2.2, at least two tooth pairs are in mesh at all times.

The Moment of Inertia and Section Modulus of the Tooth Root of a Curvilinear Gear. First, we observe the cross section of the tooth root of a spur gear. (See Fig. 5.)

The moment of inertia is

$$I_{spur} = \frac{1}{12} BS_o^3 \tag{4}$$

The section modulus is

$$W_{spur} = \frac{1}{6} BS_o^2 \qquad (5)$$

Then let us observe the cross section of the tooth root of a circular tooth gear. (Fig. 6.)

By computation, we found that its modulus W_c is bigger than W_{spur}. We tabulate the numerical value of a real example in Table 1.

For instance, if we design a pair of curvilinear gears whose $B/2R_o = 0.6$, from the table we find $W_c/W_{spur} = 1.20$ and $\Sigma E = 2.76$ (ΣE of the spur gear is only 1.7). Then the strength of such gear is $1.20 \times \frac{2.76}{1.7} = 1.95$ times stronger than the spur gear.

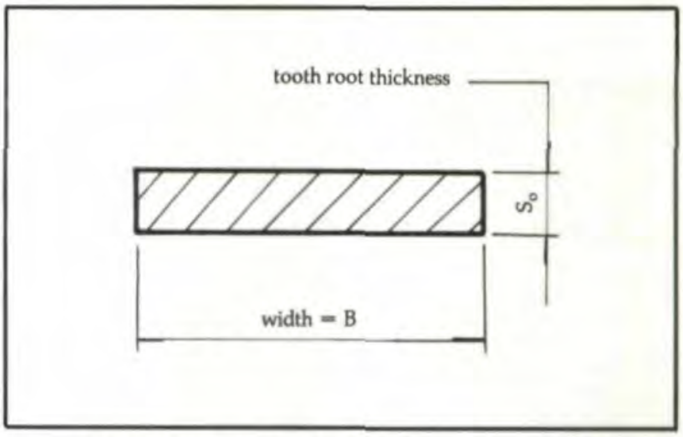

Fig. 5 – Cross section of the tooth root of a spur gear.

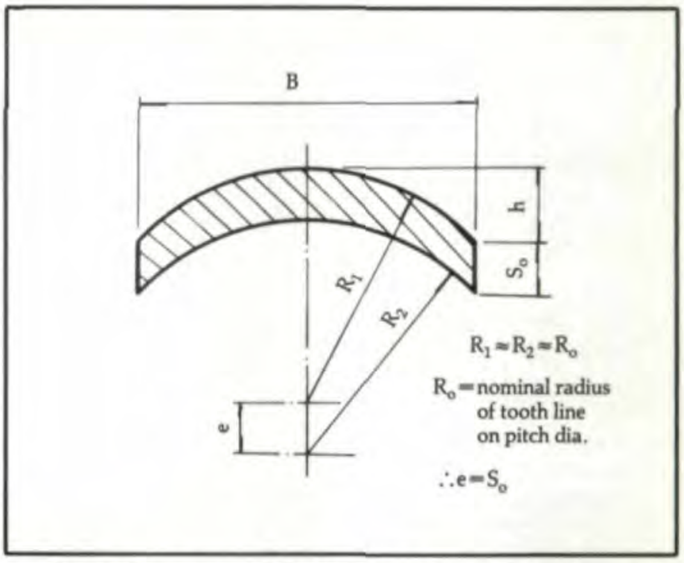

Fig. 6 – Cross section of the tooth root of a circular tooth gear.

Table 1. Moment of Inertia and Section Modulus of Circular Gear Tooth

$B/2R_o$	I_c/I_{spur}	W_c/W_{spur}	ΣE
0.50	2.52	1.059	2.55
0.52	2.64	1.076	2.60
0.54	2.79	1.105	2.64
0.56	2.96	1.139	2.67
0.58	3.14	1.173	2.72
0.60	3.31	1.20	2.76
0.62	3.53	1.236	2.81
0.64	3.74	1.275	2.85
0.66	3.93	1.304	2.90
0.68	4.18	1.344	2.95
0.70	4.48	1.395	3.0

I_c – Moment of inertia of a circular gear tooth
I_{spur} – Moment of inertia of a spur gear tooth
W_c – Section modulus of a circular gear tooth
W_{spur} – Section modulus of a spur gear tooth

ΣE is calculated corresponding to a special case if $Z_1 = 1.9$, and $Z_2 = 60$; whereas E_o of spur gear is only 1.7.

Table 2, The Comparison of Tooth Length Between Spur Gear and Circular Tooth Gear

$B/2R_o$	L/B	$B/2R_o$	L/B
0.50	1.047	0.60	1.072
0.52	1.052	0.62	1.079
0.54	1.056	0.64	1.085
0.56	1.060	0.66	1.092
0.58	1.066	0.68	1.10

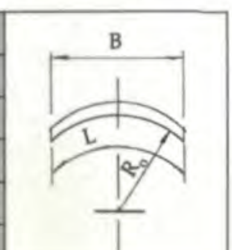

The Length of Tooth Contact Line. The length of the tooth contact line of a spur gear equals its width, but the length of tooth contact line of a circular tooth gear is somewhat longer. We may compare the two in Table 2.

The Stress Induced On a Curvilinear Gear Tooth. From this discussion, we can conclude the following:

- The bending stress of circular gear teeth is reduced by the higher contact ratio and the greater section modulus.
- The contacting stress of the circular gear tooth is also reduced by its higher contact ratio and longer length of tooth contact.
- If an alternate tooth curve is used and is approximately an arc, then it has features similar to a circular gear.

The Characteristics of Curvilinear Tooth Gears

1. Curvilinear tooth gears possess a higher bending and contacting strength; thus, the center distance of gear boxes may be reduced, while maintaining power transmissions.
2. Since there are more teeth simultaneously engaged, these gears run smoothly with low noise.
3. Oil is retained within the concave tooth surface, so there is always an oil film between the two engaging surfaces,

resulting in good lubrication qualities.

4. No axial force is produced during operation, so axial bearing load is negligible.
5. Gears with similar, but not identical, modules can be cut with a single tool set, saving tooling costs.
6. Because of the simplicity of the cutting tool, it is easy to implement carbide cutting, resulting not only in an increase in manufacturing efficiency, but also in the ability to cut gears with much higher hardnesses, producing improved quality.

At present, these gears are in use in steel plants, aluminum rolling mills, cement equipment plants and other places. Their superiority has been proven in practice. The service life of machinery has been improved by anywhere from two to forty times or more.

Editors' Note:

Gearing of this type was available in the U.S. some years ago under the name "Spuricals". The herringbone type gear, in use worldwide, also has the same attributes and would be the first choice by a gear applications engineer today. Some reasons are currently available machine and cutting tools and the availablility of some competitive gear vendors. Some of the variations in the longitudinal form of gear teeth that have been used are shown in Fig 7.

To produce these gears with proper contact, some form of profile and longitudinal adjustments may be necessary. The profile of the blades can be modified to produce tip relief or root relief on the gear tooth, and the radius of curvature of the cutters can be altered to provide a central bearing contact, avoiding tooth edge contact.

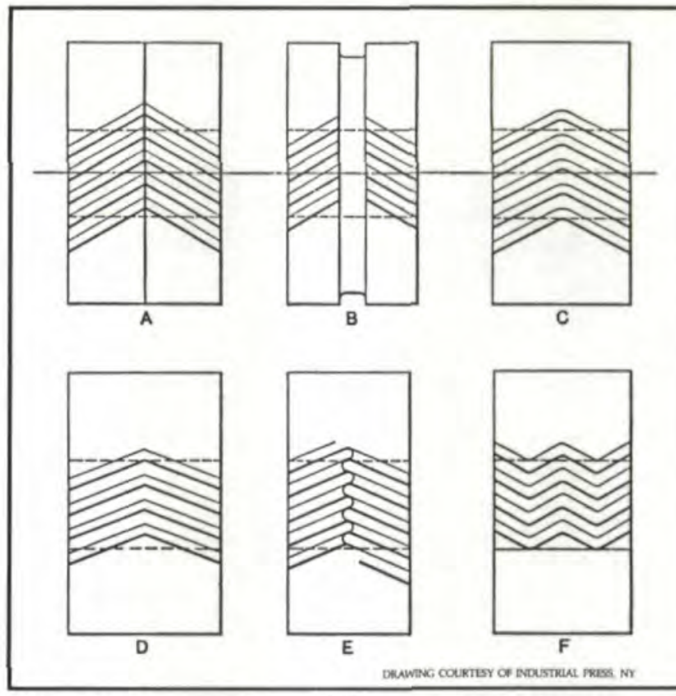

Fig. 7 – Diagrammatical views of different types of herringbone gears.

Acknowledgement: *The editors wish to thank Mr. William L. Janninck for his help with the technical editing of this article.*

Tooth Root Stresses of Spiral Bevel Gears

Hans Winter,
Technical University of Munich
Munich, West Germany
Michael Paul,
Zahnradfabrik Passau GmbH
Passau, West Germany

GEAR SPECIFICATIONS

Nomenclature	Pinion		Gear
number of teeth	11		36
normal pressure angle		20°	
normal module in midface width /mm/		12	
outer transverse module /mm/		17.50	
outer pitch diameter /mm/	192.50		630.00
mean spiral angle		34.597°	
face width /mm/		110.00	
cutter radius /mm/		210.00	
total contact ratio (theoretical)		2.8	
addendum modification	0.34		−0.34
thickness modification	0.025		−0.025
material		17 CrNiMo 6 (through-hardened)	

Variation of lengthwise crowning:

Gear Set	Cutter Eccentricity /mm/ Pinion	Gear	Contact Pattern
A	±7	0	"small"
B	±1.2	0	"large"
C	±2.5	0	"mean"

Fig. 1 – Main data of test gear sets.

Introduction

Service performance and load carrying capacity of bevel gears strongly depend on the size and position of the contact pattern. To provide an optimal contact pattern even under load, the gear design has to consider the relative displacements caused by deflections or thermal expansions expected under service conditions. That means that more or less lengthwise and heightwise crowning has to be applied on the bevel gear teeth.

In order to gain reliable information on the interrelationship between stresses, tooth crowning and relative displacements between pinion and mating gear, extension investigations were carried out by the authors. The aim of these investigations was to determine the quantitative influences of different displacements on the tooth root stresses and, by evaluating the results, to give recommendations for choosing the optimal amount of crowning.

Test Gears and Investigation Method

To measure the tooth root stresses, strain gauges were applied on the test gears. They determined the stress distribution over the root fillet and over the face width. A detailed description of the strain gauge application and measuring method is given in Reference 1. To provide enough space for the strain gauges, test gear sets having a large module had to be chosen. (Main Data. See Fig. 1.) Three sets of test gears were available, differing only in the amount of lengthwise crowning. (See Fig. 2.) The tooth profiles were kept exactly the same for all pinions and gears.

First we shall discuss the case of optimal mounting positions for the pinion and gear. By use of special features on the test rig, these positions could be maintained, even under heavy loads. Then the additional effects caused by displacements shall be described. Note that throughout the discussions, "crowning" shall always be understood as lengthwise crowning.

Influence of Lengthwise Crowning on Tooth Root Stresses

Fig. 3 shows the maximum tooth root stresses during one load cycle in the case of multiple and single tooth contact. The

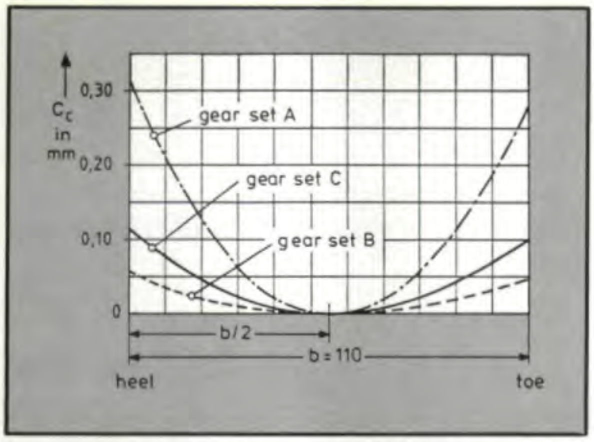

Fig. 2—Lengthwise crowning of the test gears.

stresses measured with single tooth contact (no load distribution between pairs of teeth meshing simultaneously) slightly increase with larger crowning. This obviously is an effect of the more and more concentrated load application when the size of the contact pattern is reduced by a higher amount of crowning. This can be described as a problem of load distribution over the lines of contact.

When looking at the curves for multiple tooth contact in Fig. 3, one can see that the stresses now are considerably lower than in the case of single tooth contact, especially for gear set B with small crowning and when high loads are applied. For gear set A with large crowning, there is almost no difference in stresses between multiple and single tooth contact even with high loads. Gear set C also gives a clear result: There is quite a strong influence of crowning on load distribution between neighboring pairs of teeth. In gear set A one pair of teeth has to carry almost the total load; on the contrary, in gear set B there is a considerable sharing of load between two or three pairs of teeth.

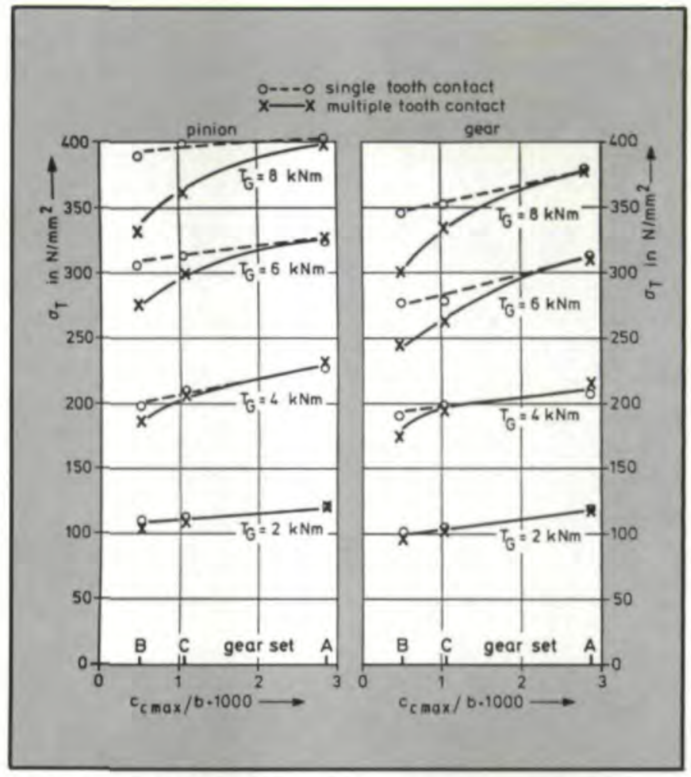

Fig. 3—Influence of lengthwise crowning on maximum tooth root stresses with single and multiple tooth contact (optimal mounting condition).

Therefore, two different problems relating to the effects

Nomenclature

b	– face width, mm
b_a	– tooth length, mm
b_{TB}	– width of contact pattern, mm
c_c	– lengthwise crowning, mm
d_m	– mean pitch diameter, mm
f	– displacement (in general), mm
f_a	– offset displacement, mm
f_v	– axial displacement, mm
f_Σ	– shaft angle deviation, degrees
g_α	– length of path of contact, mm
h	– tooth height
h_w	– active tooth height
l_B	– length of line of contact, mm
$l_{B'}$	– projected length of line of contact, mm
w	– influence coefficient for load distribution

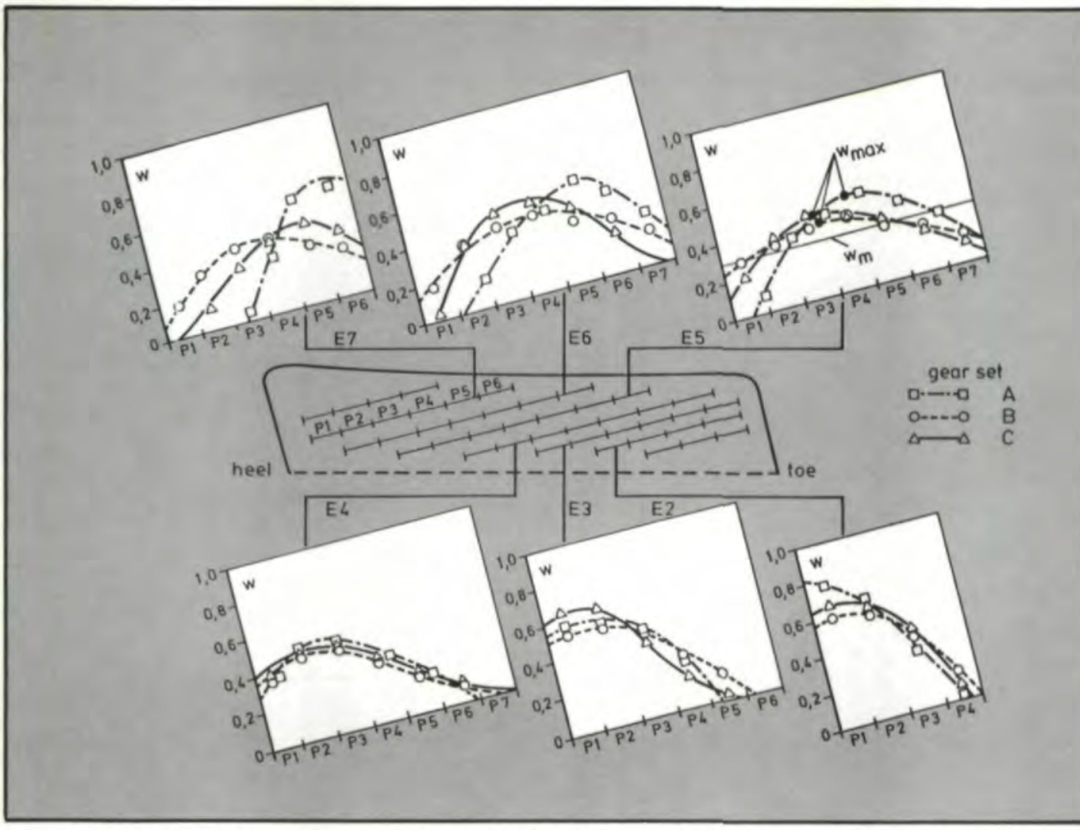

Fig. 4 – Influence of lengthwise crowning on the load distribution over the lines of contact (single tooth contact).

of crowning have to be discussed: Load distribution over lines of contact and load distribution between gear pairs meshing simultaneously.

Load Distribution Over Lines of Contact

By using the superposition principle the load distribution over the lines of contact could be determined from root stress measurements with pointwise load application on the teeth. Fig. 4 shows the results for the test gears valid for the desired

E	–	mesh position
F	–	force, N
F_{mt}	–	tangential force in mean face width, N
K_c	–	optimization factor for lengthwise crowning
$K_{F\beta-c}$	–	lengthwise crowning factor
$K_{F\beta-f}$	–	displacement factor
M	–	measure point
P	–	position of point load
R_e	–	outer cone distance, mm
R_i	–	inner cone distance, mm
T_E	–	torque (on pinion) carried by one pair of teeth, Nm
T_G	–	total pinion torque, Nm
Y_γ	–	load sharing factor
β_b	–	base spiral angle, degrees
β_B	–	inclination angle of line of contact, degree
σ_T	–	stress in depthwise direction, N/mm^2

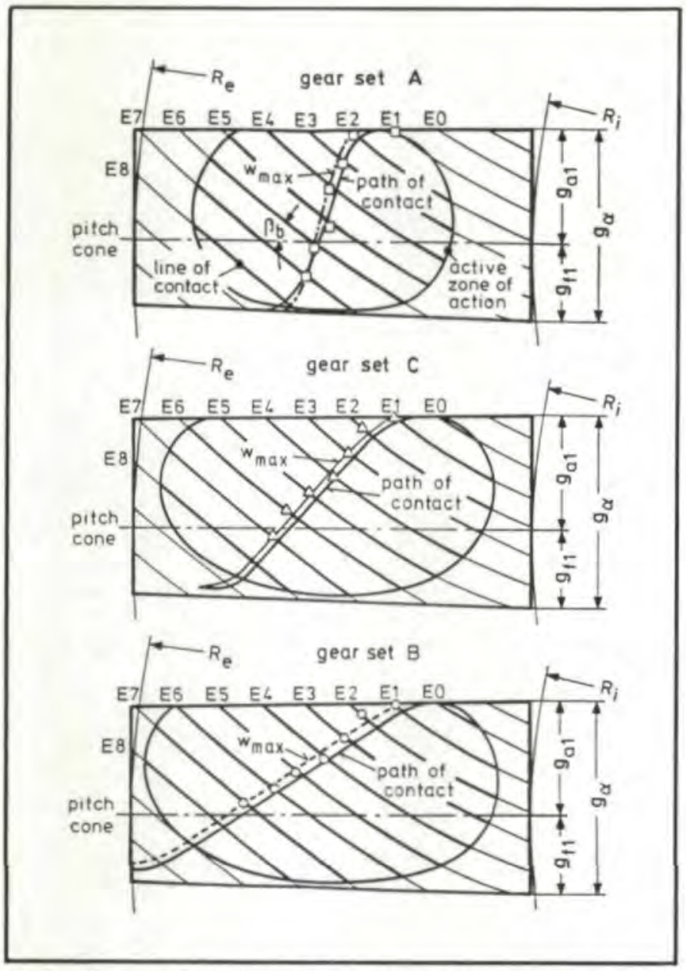

Fig. 5 – Zones of action with paths of contact and load maximum on lines of contact.

position of contact pattern. In this case, with equal surface integrals for each position, the load distribution is very unsymmetrical in the beginning (E2, E3) and the end (E7) of the contact. Only on the particular line of contact running approximately through the center of the tooth (E5) is there an almost symmetrical distribution. The gradient of this distribution depends on the amount of crowning.

This effect can be explained when looking at the corresponding zones of action shown in Fig. 5. The positions of maximum loads on the lines of contact obtained by measurements are compared with the theoretical paths of contact. There is a quite close agreement that corresponds with the theoretical idea of the Hertzian contact. This figure also explains why unbalanced load distributions must appear in the beginning and the end of the contact, while symmetrical distributions can be expected on the center crossing lines. Since bevel gears normally are designed so that the paths of contacts run through the center of the zone of action, this result may be generalized.

It has to be pointed out that the results of Figs. 4 and 5 are valid in the case of single tooth contact. In Reference 1 it was shown that the maximum stresses appear in mean mesh positions; for example, E5 in Fig. 4. So in order to find the influence of crowning on the root stresses caused by different load distributions over the lines of contact, only those mean mesh positions are of practical interest; therefore, a symmetrical load can be assumed over the corresponding lines of contact.

Based on the measurements, the influence of more or less steep load gradients was further investigated by theoretical means. Calculations using the plate theory[2,3] and the finite element method were performed with a three dimensional tooth model. In Fig. 6a the factor $K_{H\beta} = w_{max}/w_m$ describes the nonuniformity of the load application. Factor $K_{F\beta-c}$ describes the increase of tooth root stresses due to different load distributions:

$$K_{F\beta-c} = \sigma_{F\,max}(K_{H\beta}>1)/\sigma_{F\,max}|(K_{H\beta} = 1)$$

The results of Fig. 6b, which in some points are confirmed by experiment, give an overview of the influence of the maximum line load ($K_{H\beta}$) on the maximum root stresses ($K_{F\beta-c}$). It can be seen that this influence strongly depends on the portion l_B' of tooth length b_a that is covered by the line of contact. For a low ratio of l_B'/b_a there is already a

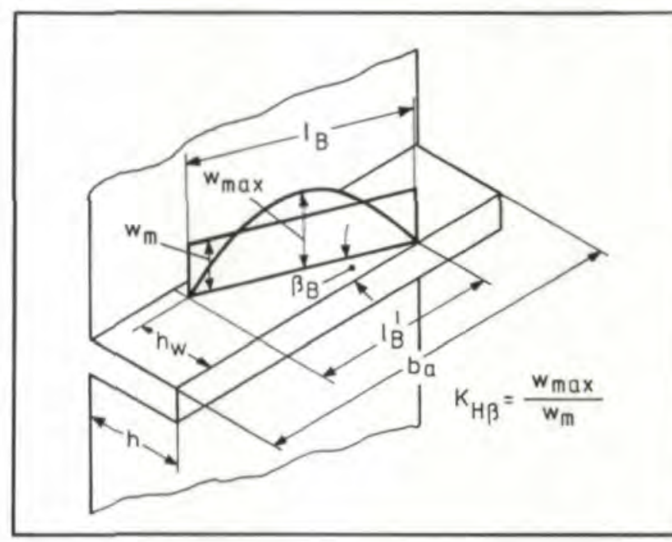

Fig. 6a – Definitions on the tooth model for theoretical calculations.

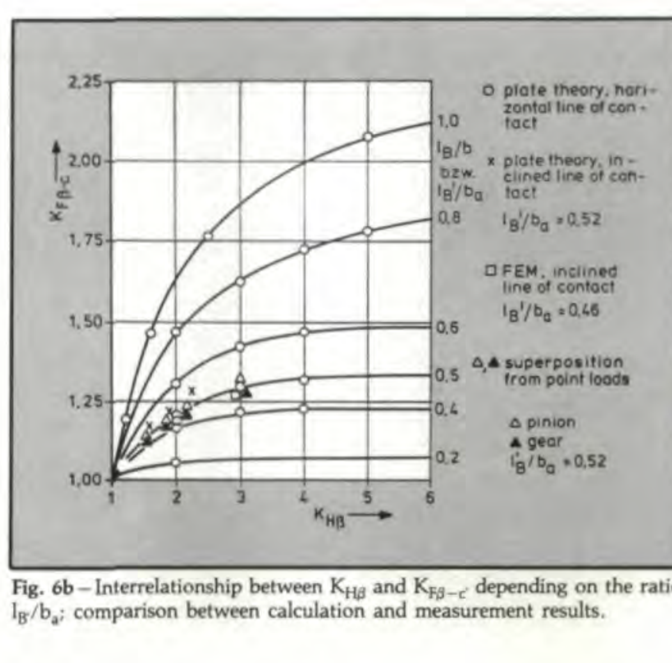

Fig. 6b – Interrelationship between $K_{H\beta}$ and $K_{F\beta-c}$ depending on the ratio l_B'/b_a; comparison between calculation and measurement results.

strong stress concentration below the short line of contact even with a uniform load distribution. In this case a more or less steep load gradient has only a minor effect. On the other hand, a large ratio l_B'/b_a is quite sensitive to load distribution.

In the case of spiral bevel gears, usually one will have a ratio of $l_B/b_a \approx 0.5$ under design load. Assuming approximately this value, the factors ($K_{H\beta}$) and ($K_{F\beta-c}$) can be plotted versus the amount of lengthwise crowning. (See Fig. 7.) This figure allows a general estimation of this effect for practical applications.

Influence of Crowning on Load Sharing With Multiple Tooth Contact

Fig. 3 already showed that the crowning effects considerably the maximum portion of load carried by one pair of teeth during one load cycle. Fig. 8 shows this effect measured with the test gear sets under two different loads.

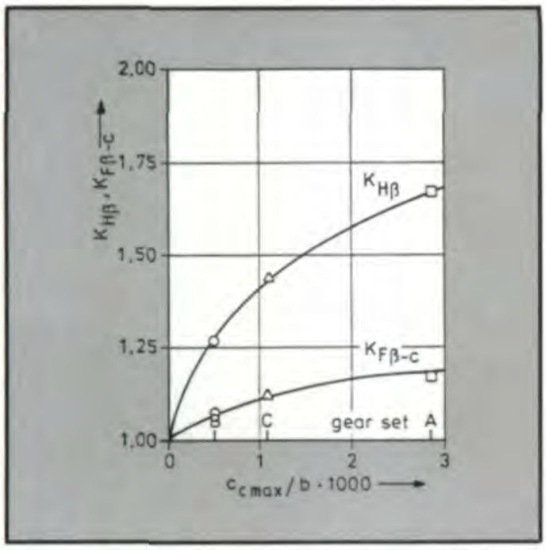

Fig. 7 – Influence of lengthwise crowning on $K_{H\beta}$ and $K_{F\beta-c}$. ($K_{H\beta}$, see Fig. 4; $K_{K\beta-c}$, see Fig. 6b.)

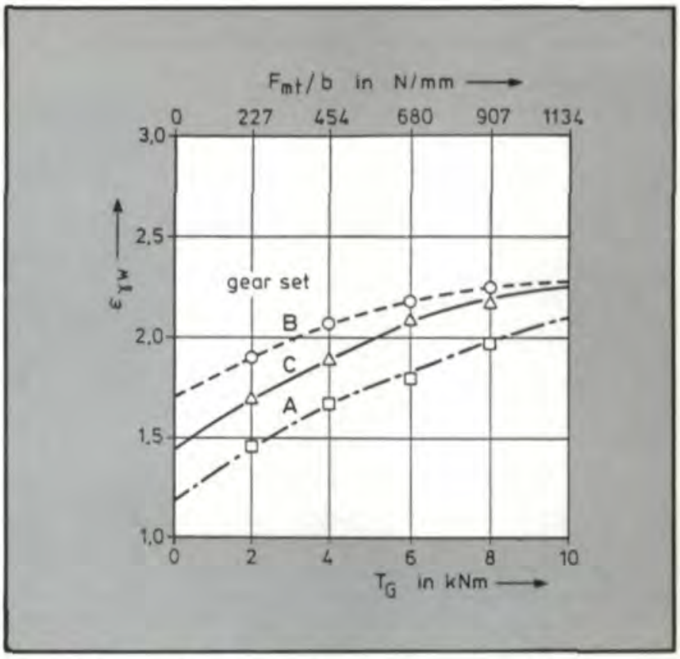

Fig. 9 – Influence of load on the effective total contact ratio measured for the test gear sets.

Looking at the low load ($T_G = 4$ kNm), one can see that for gear sets A and C (large and mean crowning) there is an area of effective single tooth contact. (One pair of teeth carries 100% load, $T_E/T_G = 1$.) For gear set B (small crowning) the maximum portion of load is about 95%.

When higher torque ($T_G = 8$ kNm) is applied only in gear set A, one pair of teeth still has to carry the total load for a short time; i.e., with this torque on gear set A just the significant value of $\epsilon_{\gamma w} = 2$ for the effective total contact ratio is reached. So from these results, the interrelationship between load, crowning and effective contact ratio can be derived. (See Fig. 9.)

It is of interest to compare the effective contact ratio determined by measurement with calculated contact ratios according to AGMA[(4)] or DIN[(5)] standards. Fig. 10a compares the values for the example of gear set A. The results show that the contact ratios according to DIN 3991 are too high over the whole torque range; and that the AGMA values fit quite well at low torques. Until higher torques are reached, the measured contact ratio increases more rapidly than the calculated contact ratio.

The differences can be explained by considering the zones of action assumed by the calculation methods. (See Fig. 10b.) The real zone of action (1) determined by experiment is smaller than the rec-

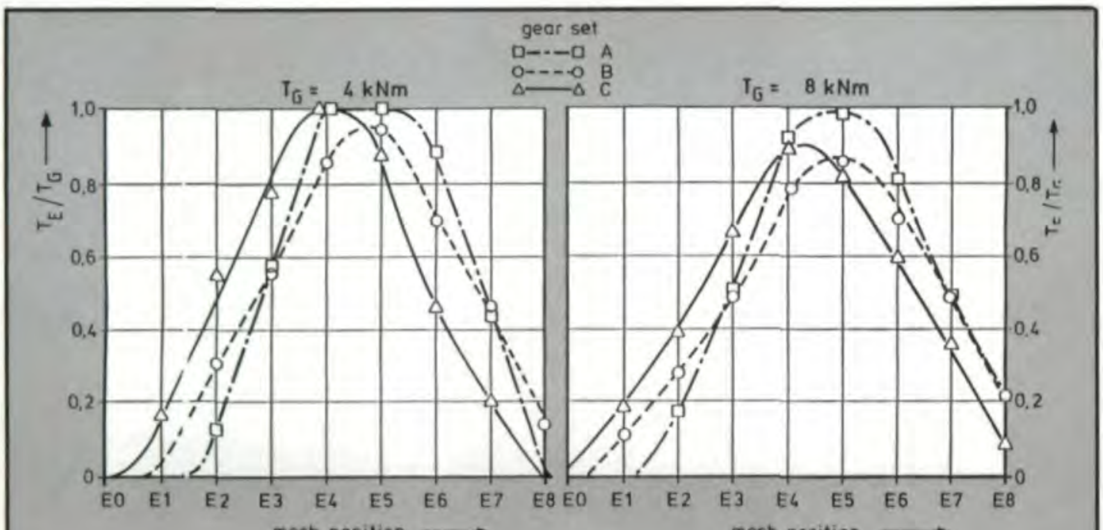

Fig. 8 – Influence of crowning on portion of load carried by one pair of teeth during one load cycle.

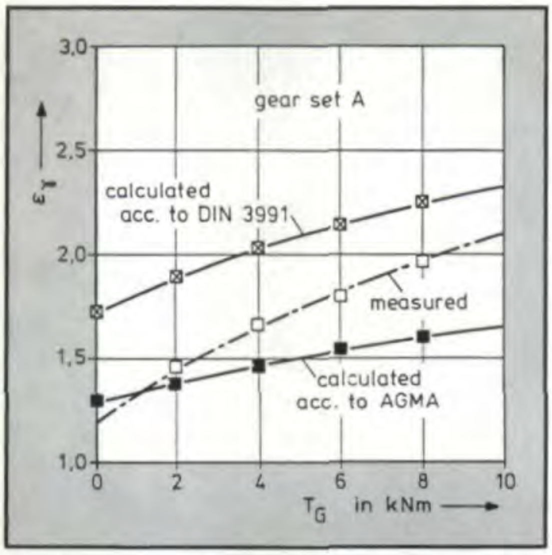

Fig. 10a – Comparison between calculated and measured total contact ratios. Example: Gear set A.

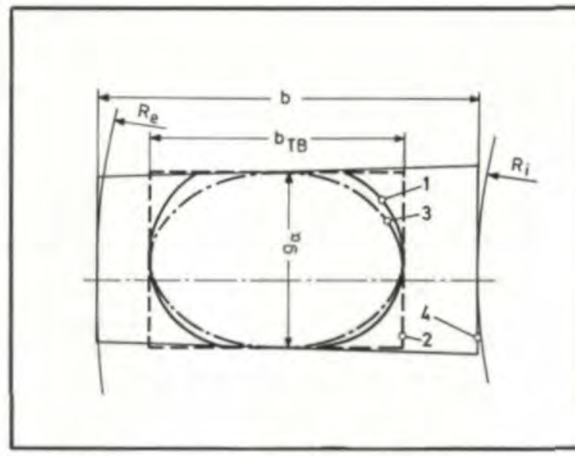

Fig. 10b – Comparison between the actual effective zone of action and the zones of action assumed by the calculation methods. Example: Gear set A. 1 – actual zone of action; 2 – zone of action for virtual cylindrical gears per DIN 3991[4]; 3 – elliptical zone of action per AGMA 2003[5]; 4 – theoretical zone of action for teeth without crowning.

tangular zone of action according to DIN (2) and larger than the elliptical zone of action asumed by AGMA (3). Correspondingly, the actual effective total contact ratio lies between the values of AGMA and DIN. Nevertheless, the shape of the real zone of action seems to be nearer to the AGMA than to the DIN assumption.

The greater increase of the measured total contact ratio in comparison with the calculated ratios results from the fact that both the DIN and AGMA calculations only consider the influence of load on the face contact ratio, but not on the profile contact ratio. Nevertheless, due to tooth deflections and the heightwise crowning, the profile contact ratio also increases with higher loads. So with regard to this effect, the curves of Fig. 10a seem plausible. A rough estimation of the influences of load and crowning on the effective total contact ratio of spiral bevel gears can be taken from Fig. 11.

With regard to the tooth root stresses, the interrelationship between contact ratio and maximum amount of load carried by one pair of teeth is of interest. Fig. 12 shows the maximum values of T_E/T_G, called load sharing factor Y_γ, versus the effective total contact ratio. One can see that the

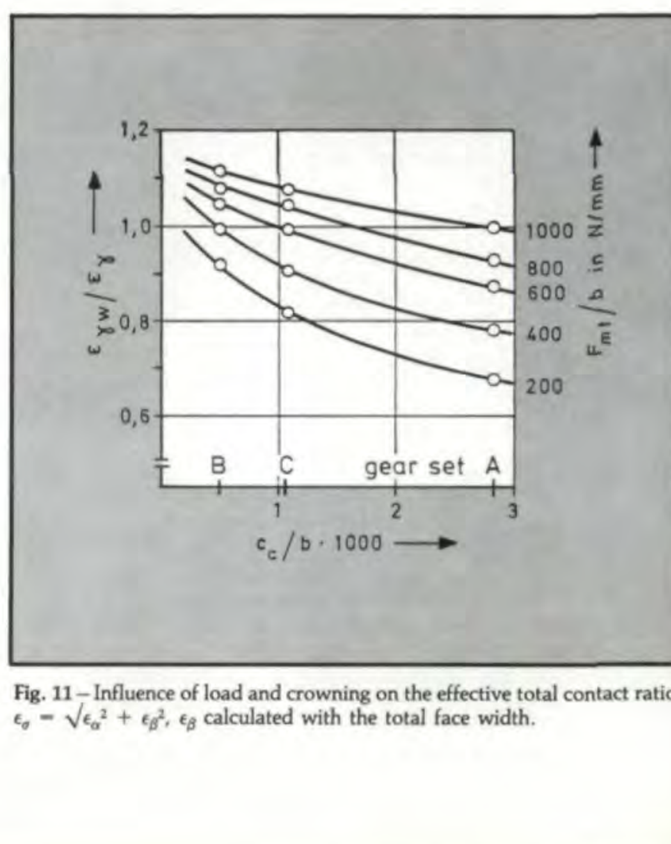

Fig. 11 – Influence of load and crowning on the effective total contact ratio. $\epsilon_\sigma = \sqrt{\epsilon_\alpha^2 + \epsilon_\beta^2}$, ϵ_β calculated with the total face width.

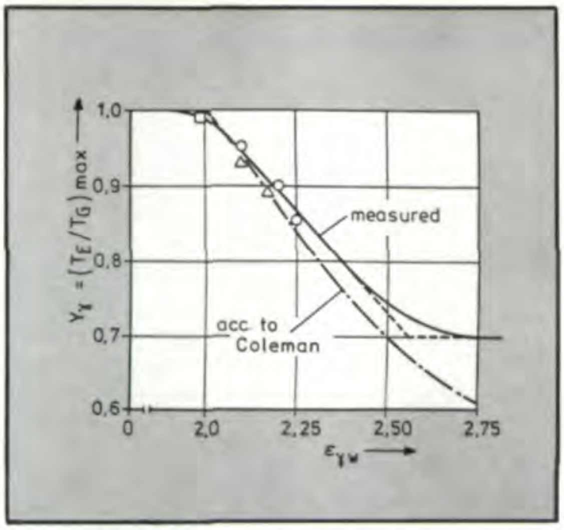

Fig. 12 – Load sharing factor Y_γ. Comparative values according to Coleman.[6]

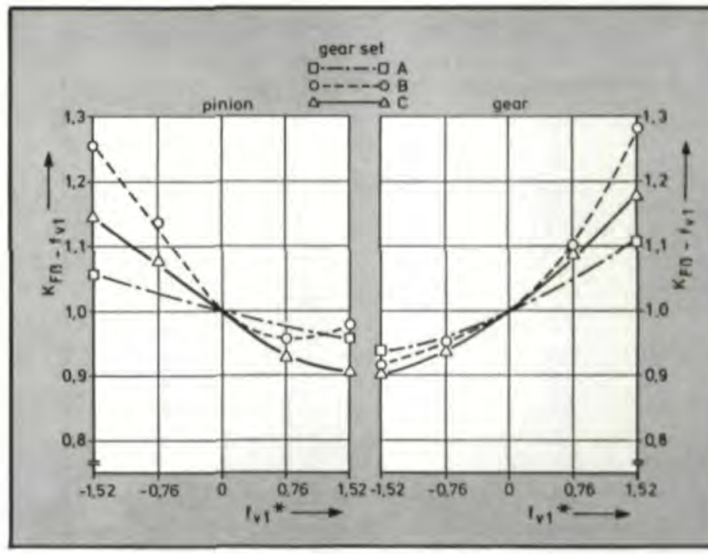

Fig. 14 – Factor $K_{F\beta-fv1} \cdot f_{v1}{}^* = f_{v1}/d_{m2} \cdot 1000$.

measuring results correspond quite well to an earlier formulation of Coleman[6] if the effective values of contact ratio are used here as well. From this investigation, we may conclude that the influence of lengthwise crowning on the tooth root stresses resulting from a differing load distribution over the lines of contact (factor $K_{F\beta-c}$), and from a differing load sharing (factor Y_γ) can be estimated quantitatively.

Influence of Relative Displacements

The results discussed before were valid for optimal positions of the contact patterns even under heavy loads; i.e., an ideal stiff configuration was simulated on the test rig. Nevertheless, under practical conditions some displacement of pinion and gear cannot be avoided. Therefore, this investigation also covers the influence of those relative displacements on the root stresses. By performing similar measurements on the three test gear sets, the effect of crowning could be considered too. Fig. 13 gives a definition of all relative displacements that can occur between pinion and gear.

To describe the difference in maximum root stresses when certain displacements are adjusted ($f \lessgtr 0$), the factor $K_{F\beta-f}$ was introduced. It is defined as

$$K_{F\beta-f} = \sigma_{Tmax}\ (f \lessgtr 0)/\sigma_{Tmax}\ (f = 0).$$

Fig. 14 shows this factor ($K_{F\beta-fv1}$) in case of axial displacements of the pinion (f_{v1}). The corresponding shapes and positions of the contact patterns on the gear teeth are given in Fig. 15. As expected, the shift of the contact pattern is stronger with a small amount of crowning (gear set B) and less with the high crowned gear set A. Of course, the variation of the root stresses is graded correspondingly.

In all gear sets for a certain value of displacement, there is a counteracting influence on the pinion and gear stresses. This is caused mainly by the opposite shift of the contact pattern in the heightwise direction on the flanks of pinion and gear. As a result, the increase of the stresses for contact patterns near the tip of the teeth is stronger than the equivalent stress decrease when the patterns are positioned barely in the root.

So far the discussion has been theoretical and does not have direct practical application. Under service conditions a single type of displacement will not appear alone. The total relative

Fig. 13 – Definition of relative displacements between pinion and gear.[7]

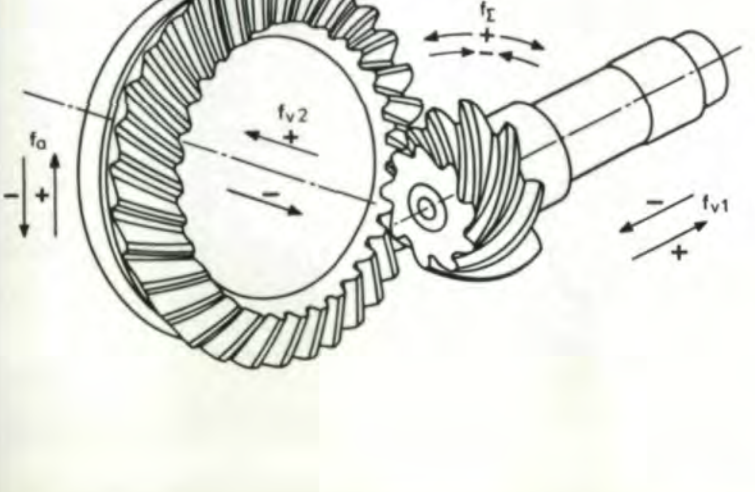

AUTHORS:

PROF. DR.-ING. HANS WINTER *is the head of the Laboratory of Gear Research and Gear Design at the Technical University of Munich. He has worked in the German gear industry since 1956 in manufacturing, development, design and research. He received his doctorate from the Technical University of Munich and studied as an associate of Prof. Dr.-Ing h.c. Gustav Niemann.*

DR.-ING. MICHAEL PAUL *is head of the department for technical calculations of Zahnradfabrik Passau GmbH, Passau, West Germany. Prior to taking this post he worked as Chief Engineer at the Gear Research Laboratory, and he has been extensively involved in the research of tooth root stresses of spiral bevel gears. Dr. Paul received his graduate degree from Technical University of Munich.*

displacement between pinion and gear will be a combination of all the portions showed in Fig. 13. From the investigation of combined displacements the following conclusions could be derived:

- Axial displacements of the gear (f_{v2}) and deviations of the shaft angle (f_{Σ}) are of minor effect on the root stresses. Within the range of displacements that have to be expected in usual gear and housing designs this effect may be neglected. This statement is valid for gear ratios larger than 3.

- Deviations in pinion mounting distance (f_{v1}) and offset (f_a) do have a strong influence. Fig. 16 shows the root stresses measured on the pinions for different combinations of f_{v1} and f_a. It becomes very clear how the gradients depend on the amount of crowning (pinions B –> C –> A).

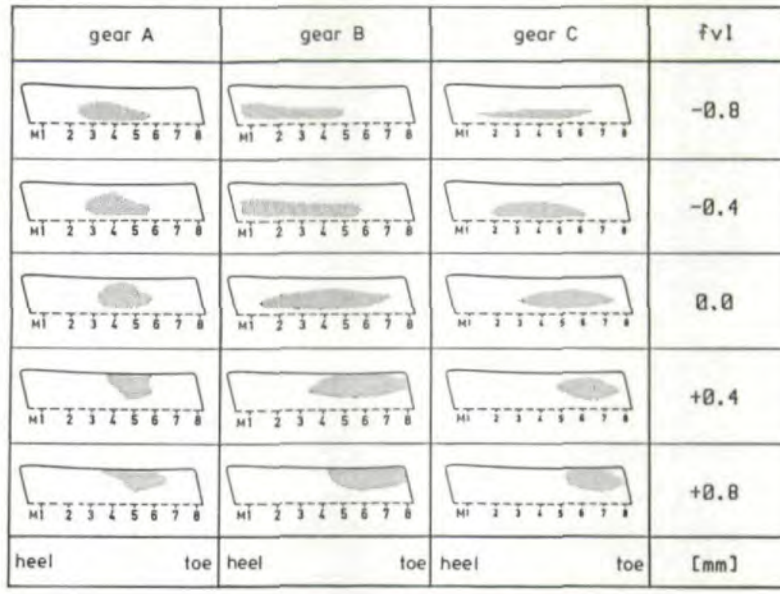

Fig. 15 – Influence of axial displacements of the pinion (f_{v1}) on the contact pattern.

- In general, determination of the factor $K_{F\beta-f}$ for a certain combination of displacements (f_{v1}, f_a) and for a certain amount of crowning (c_c) is allowed by Fig. 17. By using this factor the influence of the discussed parameters can be estimated for a given practical case.

Optimization of Lengthwise Crowning

From the knowledge of the influence of crowning and displacements discussed earlier, a criterion for the optimization of the crowning can be derived. For a given design environment with certain relative displacements (measured or

(continued on page 45)

Computer-Aided Design of the Stress Analysis of an Internal Spur Gear

Jeng-Fong Hwang
Dennis A. Guenther
The Ohio State University, Columbus, Ohio

John F. Wiechel
S.E.A., Inc.

Abstract:

Internal gearing is an important element of epicyclic gear trains. However, specific design methodology has not been adopted and the procedure for designing external gears is often employed for internal gear design. Unfortunately, internal gears differ from external gears in tooth shape and rim support, thereby complicating the stresses at critical points. The intent of the present article is to present design concepts that will accurately model the stresses in internal gears. The article employs a finite element method to investigate the effects of different parameters on the stresses of the gear. Finally, a simulation of the stress fluctuations when two gears mesh is presented.

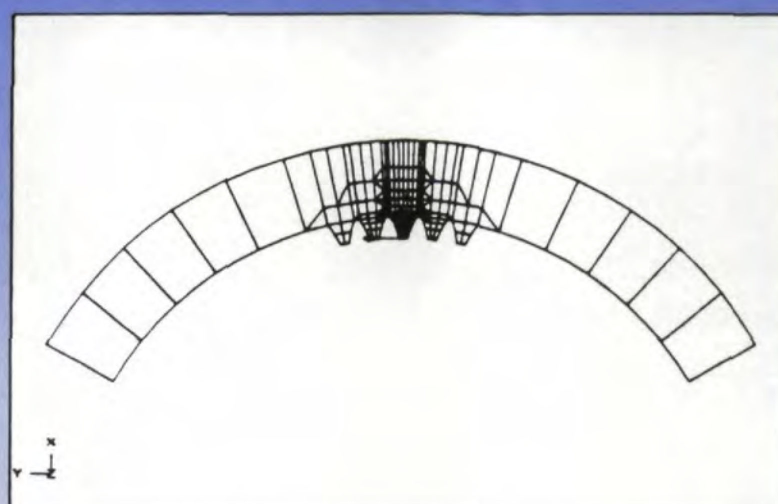

Fig. 1 – FEM model of the internal gear.

Introduction

Although there is plenty of information and data on the determination of geometry factors and bending strength of external gear teeth, the computation methods regarding internal gear design are less accessible. Most of today's designs adopt the formulas for external gears and incorporate some kind of correction factors for internal gears. However, this design method is only an approximation because of the differences between internal gears and external gears. Indeed, the tooth shape of internal gears is different from that of external gears. One has a concave curve, while the other has a convex curve. Usually, internal gear teeth are thick at their base, and tooth height is short. These two characteristics make the use of the Lewis beam model for the calculation of the stresses improper, because the beam model assumes the gear tooth is a long cantilever beam, and the bending stress at the root is the dominant factor. However, for internal gears the stress distribution around the root fillets is very complex. Factors such as rim thickness, rim support conditions, root fillet radius and loading positions, must all be taken into account when accurate stress estimation of internal gears is required. Therefore, in order to meet the demand of today's high performance gear design, more information on the effects of those parameters and a more useful design concept with better numerical results should be investigated.

The work presented here provides more information about the behavior of internal spur gears under specific situations. Those areas examined were:

a. The effects of rim thickness on the root fillet stress and the whole stress distribution,
b. The effects of fillet radius on root fillet stresses,
c. The effects of loading position,

AUTHORS:

MR. JENG-FONG HWANG *is a graduate of the National Taiwan University of Mechanical Engineering and received his Masters of Engineering degree from the Ohio State University in both Welding Engineering and Mechanical Engineering. His major area of emphasis has been in computer aided design (CAP/CAM) and stress analysis using the finite element method.*

DR. DENNIS A. GUENTHER *is an Associate Professor of Mechanical Engineering at The Ohio State University where he has served since receiving his Ph.D. in 1974. He has done extensive work in the area of failure analysis and identification of failure mode, having investigated and analyzed virtually all*

d. The effects of support condition,
e. The effects of different pressure angles on the root fillet stresses.

Analysis

In the past decade, the finite element method (FEM) has been heavily used in the stress analysis of gears and has shown promising results. Drago and Pizzigati[1] have done extensive research of gear stress problems using finite element methods and have found that FEM is a good approach to investigating the rim effect on tooth fillet stresses. Moreover, it can also be used to establish stress history by subsequently changing tooth contact loading conditions for a number of points along the line of action. In this way, a quasidynamic simulation can be obtained; also the mean and alternating stresses can be calculated for each section and the critical section in fatigue can be determined. The two dimensional FEM is relatively simple to apply and is satisfactory for thin and flat gears. Drago[1] showed that his FEM results were about 12% higher than the calculations reported by AGMA.[2-5]

In the present study, the internal spur gear has been transformed into a finite element model as shown in Figs. 1 and 2.

To reduce computational costs, only a section of the gear is modeled and only the teeth in the vicinity of the loaded tooth are included. This model employed two kinds of elements, the first being a thin shell parabolic triangle, and the second, a thin shell parabolic quadratic element with the uniform thickness of 2.54 cm (1"). Basically, the models of various cases have about 800 nodes and 250 elements. In all, a total of 79 cases were tested with 162 to 261 nodes and 559 to 869 elements for the different cases. Additional detail is given by Hwang.[6]

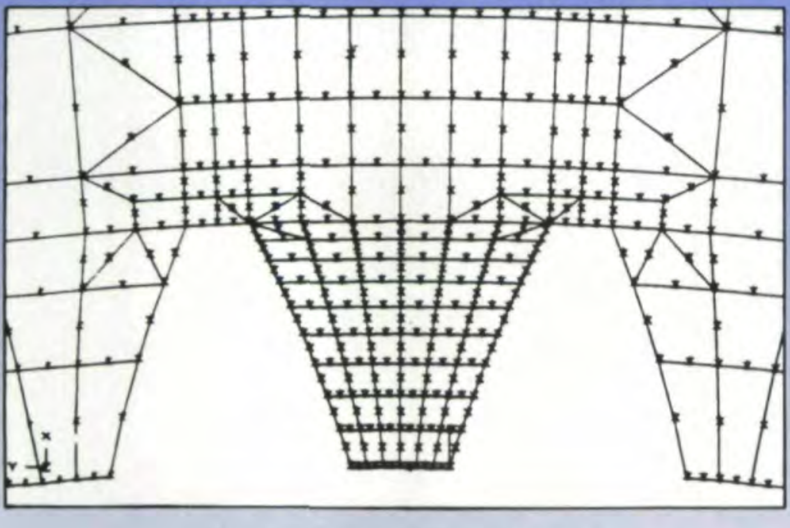

Fig. 2—FEM model of the internal gear.

The finite element analysis was carried out through the computer facility at the Advanced Design Method Laboratory (ADML), in the Department of Mechanical Engineering of The Ohio State University. The establishment of the FEM model and finite element calculation of this research were conducted through the software package, I-DEAS, running on DEC VAX 11/750 computers.

Because of the nature of the finite element method, the accuracy of the results depends very much on the mesh design of the model. Based on the study of Drago,[1] very coarse meshes will give poor results around the tooth fillet area. The best results can be derived only through several experiments of the element size and the aspect ratio of the elements used around the fillet area.

In order to assure that the mesh design and element type used can yield accurate results, verification of the model must be conducted. This model verification was carried out through the comparison of the FEM calculation in this research and the FEM and experimental results of Aida.[7] Aida's FEM model employed 1251 nodes and 2122 elements based upon a thin shell linear triangular element. He also conducted photoelasticity experiments for the verification of his model. The finite element models of this study were then established and based upon the same gear dimensions specified by Aida.

It should be noted that since the load is applied at the tooth tip and the tip is far away from the tooth root, the effect of the point load singularity upon the root fillets is minimal and can be neglected. Therefore, in the FEM model, the mesh surrounding the point load region was not modified. At the root fillet areas, the element density has significant influence on the accuracy of the results. Type, size and aspect ratio of the elements in these areas should be carefully examined. Within this study, the FEM model was established to reflect the general trends of the stress responses corresponding to different parameters of internal spur gears. The mesh and the elements used are shown in Fig. 2. This model derived the fillet stress data in the average sense over the root regions similar to the data based upon strain gage measurements. The boundary condition imposed upon this model is that the section is fixed at both ends.

The results of two FEM analyses and experimental data are presented in Fig. 3. They indicate that the results of the tensile root fillet were better than Aida's model, and the error is about 13%. However, the compressive root fillet gave worse results than that of Aida's model, but the average error was still

(continued on page 26)

phases of machinery failures. His research and teaching efforts in recent years have centered on system dynamics, design of machine elements, computer aided design, vehicle dynamics, and accident reconstruction. His interest in gear design has grown out of involvement with teaching machine design and evaluation of gear failures.

DR. JOHN F. WIECHEL *is a project engineer with S.E.A., Inc. in Columbus, Ohio. He received his B.S. and M.S. degrees in mechanical engineering from Purdue University and a Ph.D., from The Ohio State University. Reconstruction of vehicular and machinery accidents constitutes the majority of his current work with a focus on locating, identifying, and analyzing failed machine components and evaluation of the potential of the failure to produce injury.*

IMAGIN

CIMA USA's 160 *CNC6.*

NATION

It isn't hard to imagine why the legacy of Leonardo Da Vinci is alive and well at CIMA USA. Leonardo's fascination with gears, motion, and economy of design is part of our Italian heritage. It's the inspirational force behind every piece of hobbing equipment we build. And it keeps our imagination poised to transform ideas that look good on paper into machines that perform brilliantly on the floor.

CIMA Imagination Is Geared Toward Accuracy.
For accuracy, productivity, and high speed, CIMA's 160 is on the cutting edge. With 5DP capability and 6 axes of adjustment, it was designed specifically to cut gears up to 6.5" in diameter for the automotive industry. The extra precision that smaller gears require called for extra stability in our design. So we built the 160 with enough heft to eliminate vibrations, for stabler cuts and longer tool life. Plus, the motor is connected directly to the work area, effectively cancelling torsion stressors.

But the real mark of CIMA imagination is in the hob column and tail stock. A special stabilizing adaptation in these areas helps decrease distortion and increase accuracy beyond your wildest imaginings. While increasing production up to 25%. No other machine can do it because no other company has the technology. Or the imagination.

Imagination To the Nth Degree.
Fluctuations in temperature by as little as (.01) degree will result in a less than perfect gear profile. That's why we designed the 160 with our patented thermal compensation system. The system keeps the relationship between the part and hob constant. So, unlike other machines, the 160 gives you accuracy to the nth degree. Instead of in varying degrees.

Expanding The Limits Of Our Imagination All The Way To The USA.
With CIMA as your gear hobbing machine company, you're not limited to Italian manufacturing standards. Now, all of CIMA USA's equipment is built in our American factory to your American standards. Giving you access to spare parts and service as well as the most imaginatively designed hobbing equipment on the continent.

More important, CIMA won't limit your imagination. You'll find that we're as adept in the art of listening as the science of engineering. Some of our best machines, in fact, were sparked by customers' ideas. Which goes to prove that when it comes to imagination, there's a little Da Vinci in everyone.

Circle us on the reader card for more information. Or, better yet, call today and tell us exactly what your needs are. Because at CIMA USA, we can build whatever you can imagine. That's imagination!

CIMA USA
Putting Powerful Ideas In Gear.
Division of G.D. P.M., Inc.
501 Southlake Boulevard
Richmond, Virginia 23236
(804) 794-9764
Telefax (804) 794-6187 • Telex 648-4252

Leonardo Da Vinci.

Leonardo Da Vinci took an imaginative leap into the future with renderings of labor-saving machines that utilized gears and pulleys.

BOOTH NO. 6691
IMTS
The world of manufacturing technology

CIRCLE A-10 ON READER REPLY CARD

COMPUTER-AIDED DESIGN . . .

(continued from page 23)

13%. Therefore, the overall performance of the model can be regarded as satisfactory, and the same mesh design as well as the element types can be applied to other cases. This comparison has laid the foundation of the FEM model employed for the parametric study presented here.

Effects of Rim Thickness. Usually internal gears have their rim thickness relatively thinner than that of external gears and, unfortunately, the rim thickness does affect the total stress distribution. Therefore, it is worthwhile to study its influences. Fig. 4 presents the FEM results of the minimum and maximum principle stresses at root fillets of the internal spur gear under the influence of different rim thickness for a pressure angle of 20°. As the rim thickness becomes thinner, the stresses at the tensile root stay nearly the same or go up a little; however, the compressive root increases its stress significantly. This effect is especially apparent when the rim thickness is less than 4/P (P=5 in the current study). If the rim is thick, the stresses at the root fillet converge to specific values.

The explanation is that when the rim is thin, the whole rim is not rigid enough. Therefore, the rim deforms as shown in Fig. 5, and this creates high tensile stresses at the outside fiber of the rim and high compressive stress at the inner fiber of the rim (which is around the root fillet areas of teeth). At the tensile root, the tensile stress due to tooth bending is cancelled by the compressive stress generated by rim bending. However, if the rim is thick, it is very hard to bend because of its high rigidity. The whole model can be described as similar to a cantilever beam, and the root fillet stresses approach constant values. Fig. 6 shows the corresponding Von Mises stresses of the case presented in Fig. 4. Figs. 7 through 9 are the maximum principle stresss distribution within gears. Figs. 10 through 12 shows the minimum principle stress distribution. Little difference was found in stress distributions for rim thicknesses of 8/P and 6/P. The location of maximum principle stress at root fillets will tend to move to the bottom of the tooth space apart from the loaded tooth as the rim becomes thinner.

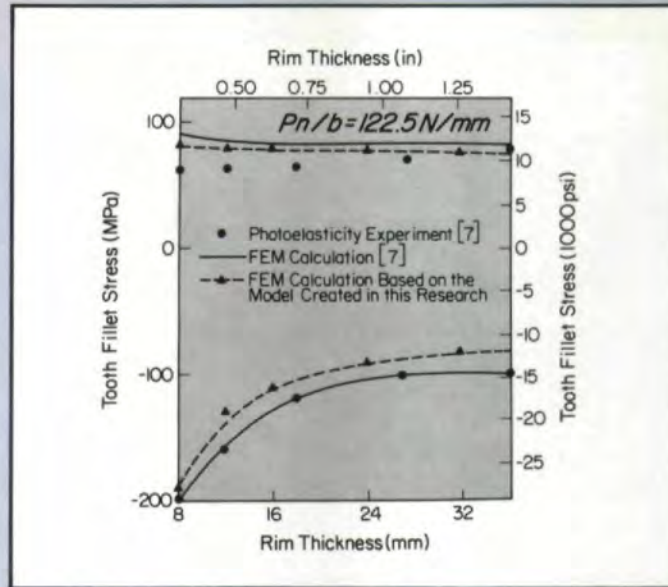

Fig. 3 – Comparison of the results based on FEM calculations of different mesh designs and experiment.

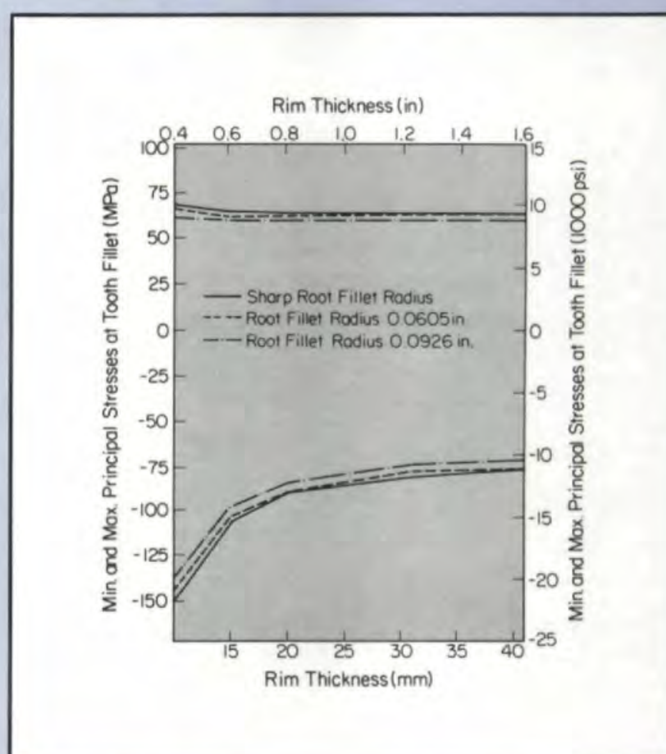

Fig. 4 – Root fillet principal stress of internal gears (ϕ = 20) with different rim thickness and fillet radii.

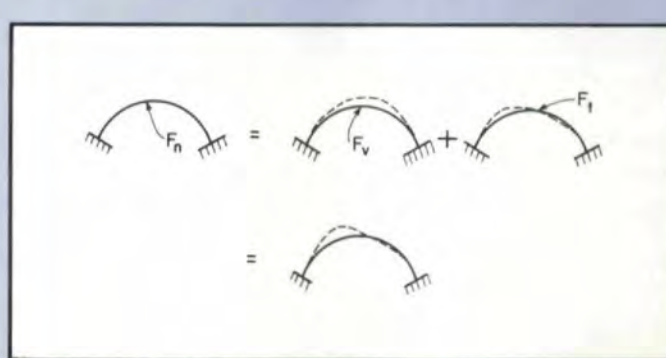

Fig. 5 – Schematic illustration of rim bending model.

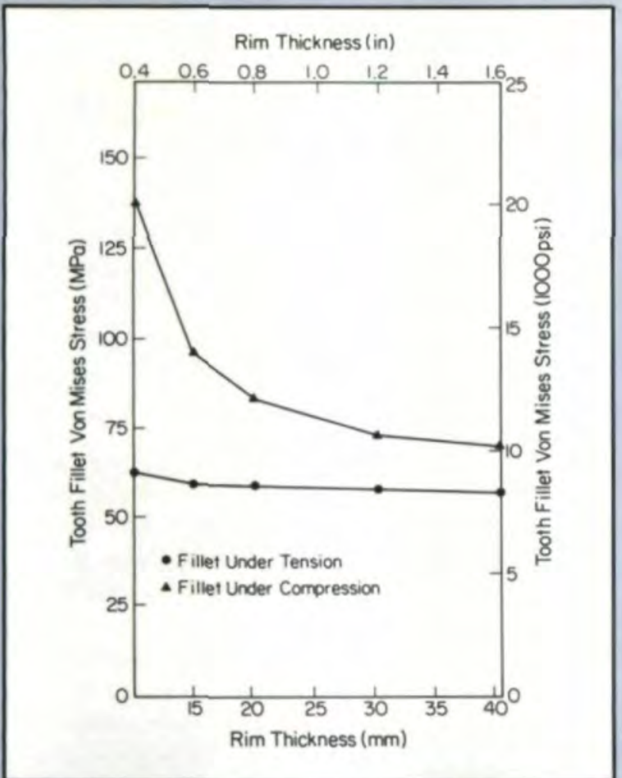

Fig. 6 – Root fillet Von Mises stresses of internal gears ($\phi = 20$) with different rim thickness and fillet radii.

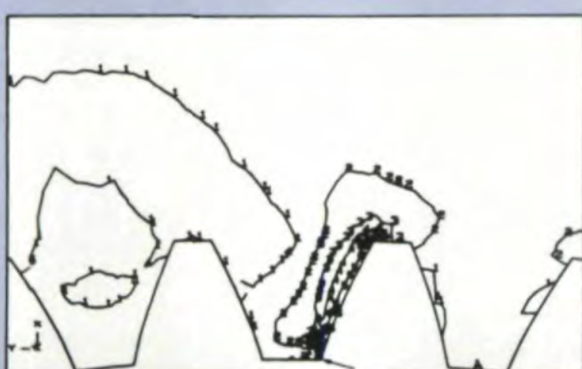

Fig. 7 – Maximum principal stress distribution of the internal gear ($\phi = 20$, rim thickness $= 6/P$).

Fig. 8 – Maximum principal stress distribution of the internal gear ($\phi = 20$, rim thickness $= 4/P$).

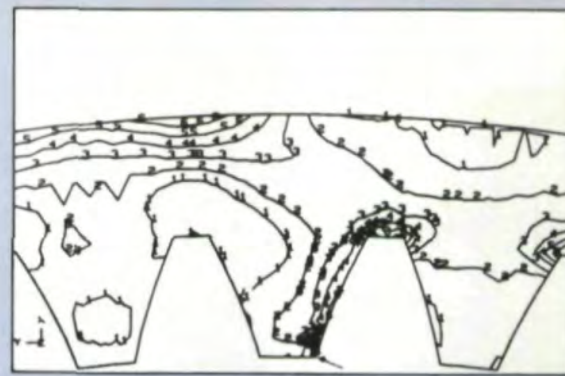

Fig. 9 – Maximum principal stress distribution of the internal gear ($\phi = 20$), rim thickness $= 2/P$).

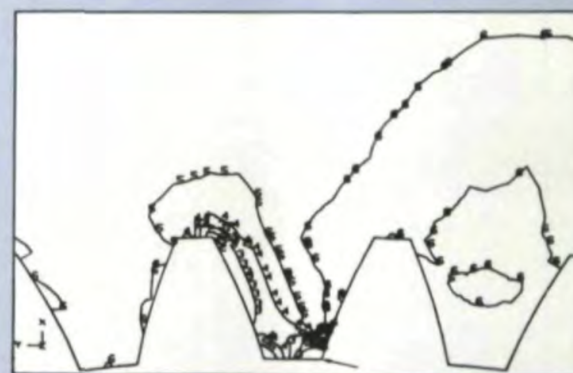

Fig. 10 – Minimum principal stress distribution of the internal gear ($\phi = 20$, rim thickness $= 6/P$).

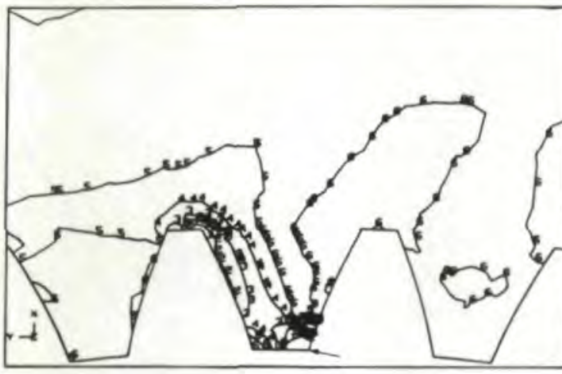

Fig. 11 (Left) – Minimum principal stress distribution of the internal gear (ϕ = 20, rim thickness = 4/P).

Fig. 12 (Right) – Minimum principal stress distribution of the internal gear (ϕ = 20, rim thickness = 2/P).

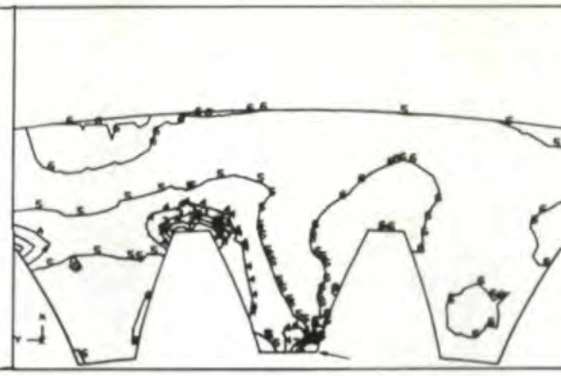

As the rim becomes thinner, the neighboring teeth are also subject to higher stresses. In other words, due to the severe bending of the rim, high stresses are built up within the rim near the loaded tooth. Under such situations, the maximum stress or the critical area may be located in the rim. The deformation of the loaded tooth and the whole rim is shown in Figs. 13 and 14 (rim thickness = 8/P), and Figs. 15 and 16 (rim thickness = 2/P). The model should contain more teeth in order to get better results for the case of a very thin rim.

Effects of Root Fillet Radius. Root fillet radius is the major factor that determines the extent of local stress concentration and is the deciding factor for the local stress magnitude. For external gears, a larger fillet radius has a local stress level smaller than that of a small fillet radius. The effect is very significant. However, in this research, the effect of fillet radius showed the same trend, but was not as pronounced because of the mesh design at the fillet areas. More accurate and detailed information should be gathered based upon comprehensive FEM modelling together with experimental verification. Aspect ratio and element density will be the key factors in this effort.

Effects of Loading Positions. When two gears mesh, the contact point will follow the path of the line of action and for each tooth in mesh, the force transmitted will be normal to the tooth surface and subsequently move along the involute profile. A simulation of the tooth stress variation can be made if subsequent loads at different positions on the tooth profile are applied to the model, and the fillet stress is calculated by FEM. This study has selected five positions along the profile to carry out this simulation as indicated in Fig. 17. At all positions, the tangential component of the

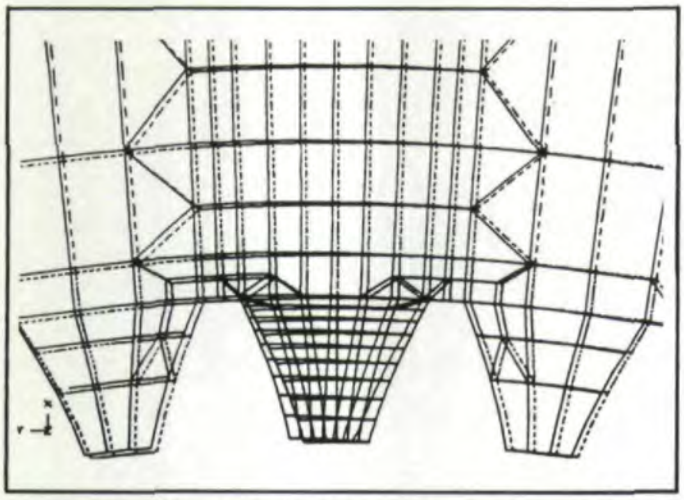

Fig. 13—Deformation of teeth ($\phi = 20$, rim thickness = 8/P).

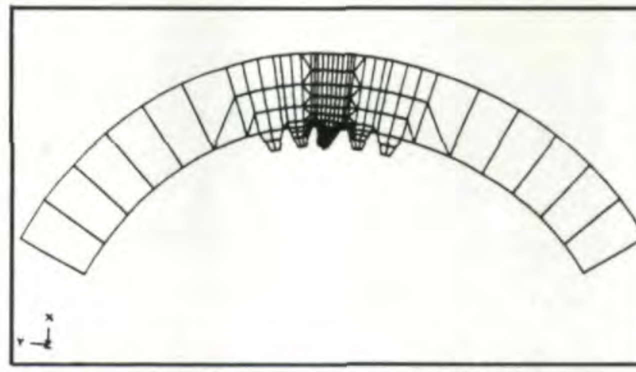

Fig. 14—Deformation of rim (ϕ = 20, rim thickness = 8/P).

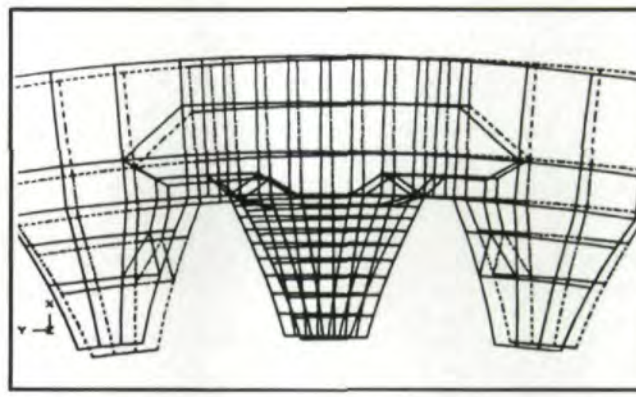

Fig. 15—Deformation of teeth ($\phi = 20$, rim thickness = 2/P).

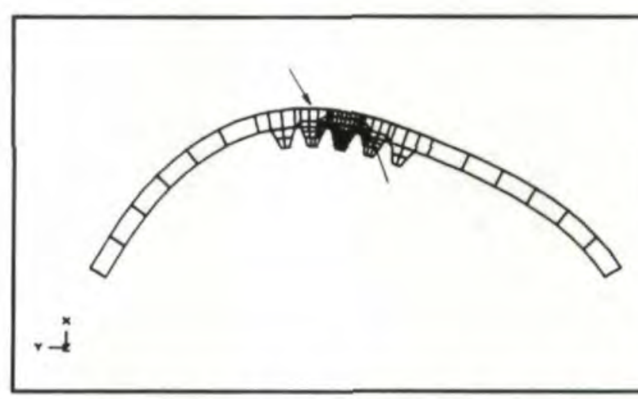

Fig. 16—Deformation of rim (ϕ = 20, rim thickness = 2/P).

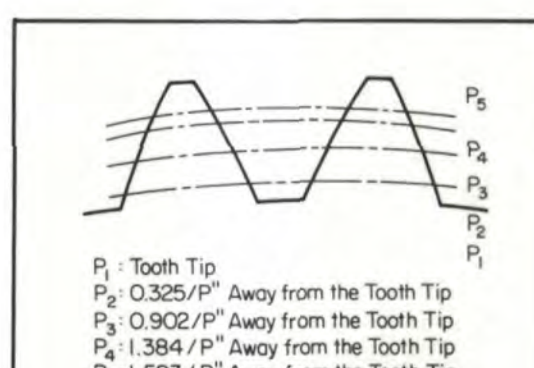

Fig. 17—Different loading position on a tooth.

load remains constant. Fig. 18 demonstrates the effect of different loading positions. As those curves show, the variation of the stresses at both tensile and compressive fillets is essentially linear unless the rim thickness is very thin. The explanation follows.

The stress due to tooth bending is linearly proportional to the bending moment. In this study, the tangential force component, which is the main factor determining the bending moment, stays the same; therefore, the bending stress is directly proportional to the moment arm. The moment arm is the distance between the tooth root and the location where load is applied. A linear relationship is thus expected.

Rim bending also makes a contribution to resultant stresses, but unless the rim thickness is thin, the effect is very limited. For thin rim cases, the deformation of rim and the rim bending stresses are very sensitive to the applied load. Some nonlinear variation due to the complicated rim deformation occurs, and it also nonlinearizes the variation of the resultant stresses. Figs. 19 and 20 show the fillet Von Mises stress for the cases in Fig. 18. Figs. 21 and 22 show the maximum principle stress distribution of the gear loaded at different positions. The stress patterns in the rim and neighboring teeth are the same except for the difference in magnitude. However, the stress distribution within the loaded tooth changes acording to the loading positions. The location of the maximum stress behaves the same way as the rim thickness effect does; namely, as the loading position approaches the root fillet, the point of maximum stress shifts its location to the bottom of the tooth space apart from the loaded tooth. The loading position effect also shows its influence the same way for those cases with different support conditions.

Effects of Support Condition. The support condition for a section of an internal gear will be dependent upon how many bolts are used in mounting the gear. The model used within this research is a section spanning two neighboring bolts cut out from the whole gear. At both ends, the boundary condition is assumed totally fixed. Four sections spanned by 60°, 80°, 100°, and 120° were analyzed. The variation of the support condition showed no obvious effect on the fillet stress. However, the variation of the support condition does have significant influence on thin rim gears.

If the span is small, the rim is rigid and, consequently, the fillet stress will be small. As the span increases, the rim becomes more flexible and the fillet stress will then increase accordingly. Especially for the compressive fillet as shown in Figs. 23 and 24, the stress magnitude may increase by 30%. The reason is that if the rim is thick enough, the whole rim is very rigid and the loaded tooth is very similar to a cantilever beam. Even though the support condition changes, the stress does not increase appreciably unless the total span between two ends is very large. For thin rim cases, the rim deformation is important and the change of the support condition will easily affect the rigidity of the rim as well as the fillet stresses.

Effects of Pressure Angle. Three different pressure angles were investigated in this study, specifically 14.5°, 20°, and

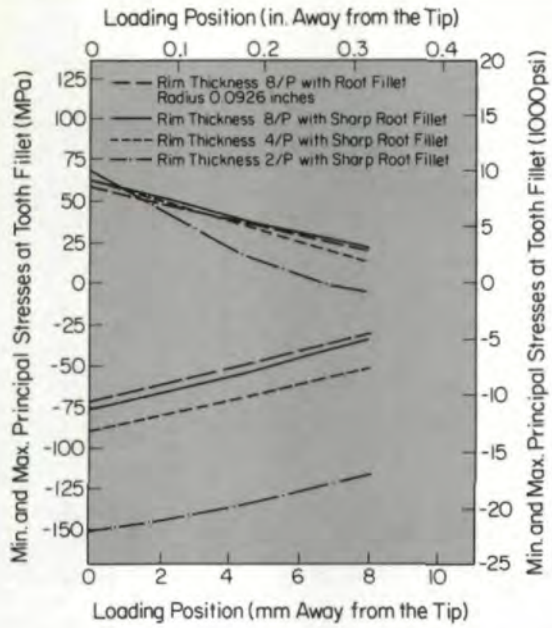

Fig. 18—Root fillet principal stresses of internal gears ($\phi = 20$) with different rim thickness and loading positions.

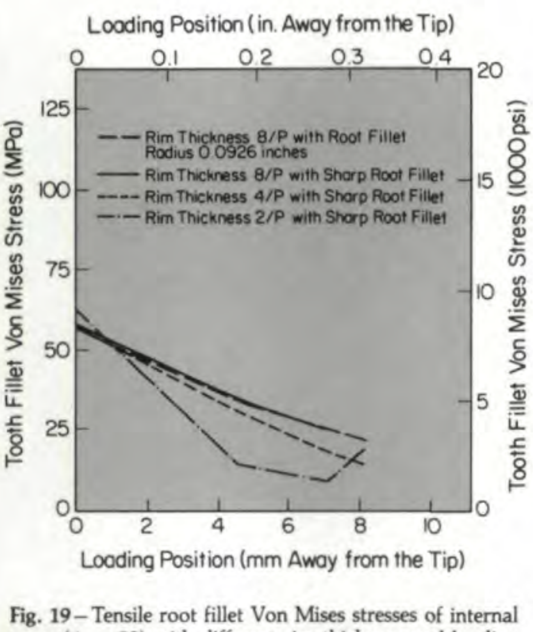

Fig. 19—Tensile root fillet Von Mises stresses of internal gears ($\phi = 20$) with different rim thickness and loading positions.

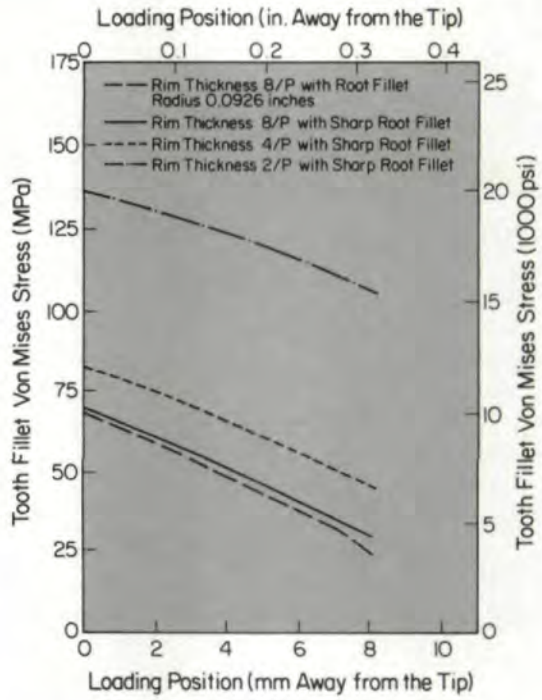

Fig. 20—Compressive root fillet Von Mises stresses of internal gears ($\phi = 20$) with different rim thickness and loading positions.

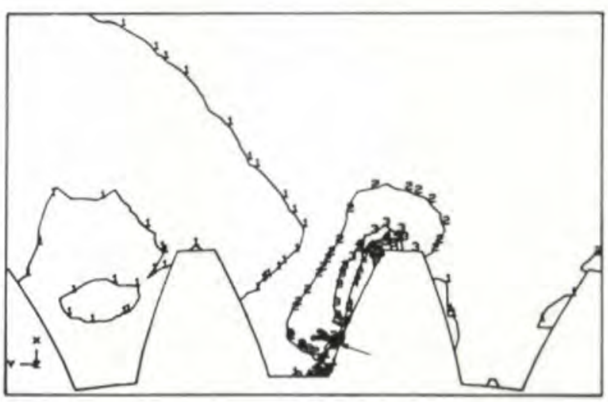

Fig. 21—Maximum principal stress distribution of internal gear ($\phi = 20$, rim thickness = 8/P) loaded at 0.325/P from the tip.

25° angles. Usually, the large pressure angle gear can sustain a larger load transmitted because a larger cross sectional area exists at the root section. Therefore, for the same loading, smaller stresses are expected. Figs. 25 and 26 substantiate this phenomenon. When the rim thickness is larger than 4/P, the larger the pressure angle, the smaller the root fillet stresses. However, if the rim thickness is less than 4/P, then, as the pressure angle increases, the stresses also increase. Rim bending is the probable cause of this phenomonen. For a rigid rim, the loaded tooth is similar to a cantilever beam, and the stress is then determined by the root cross sectional area.

As discussed previously, there are many parameters that affect the stress distribution of internal gears. Although these effects vary, each parameter has the same influence on internal gears regardless of pressure angle.

Conclusions

Other Approaches To Static Stress Analysis of Gears. Although the finite element method has frequently been applied to gear stress analysis, it usually is expensive in terms of CPU time and man-hours required to establish or edit the model. Besides, FEM can only give approximate results rather than exact

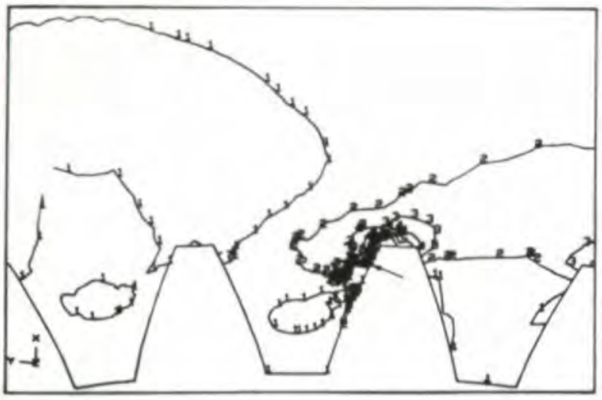

Fig. 22 – Maximum principal stress distribution of internal gear (ϕ = 20, rim thickness = 8/P) loaded at 1.593/P from the tip.

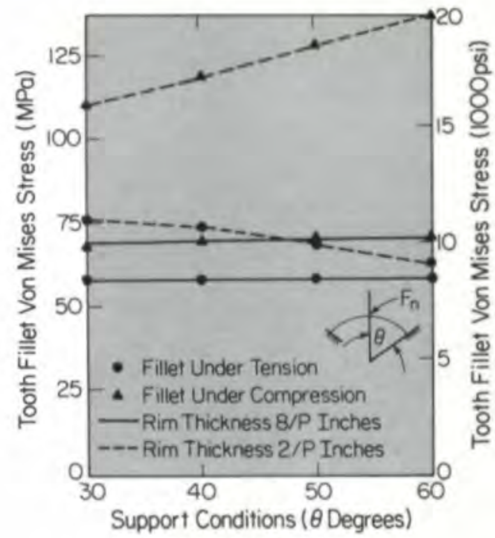

Fig. 24 – Root fillet Von Mises stresses of internal gears (ϕ = 20) with different rim thickness under various supports.

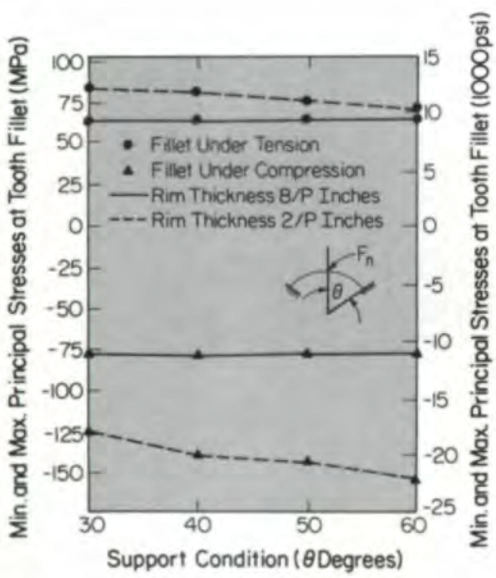

Fig. 23 – Root fillet principal stresses of internal gears (ϕ = 20) with different rim thickness under various supports.

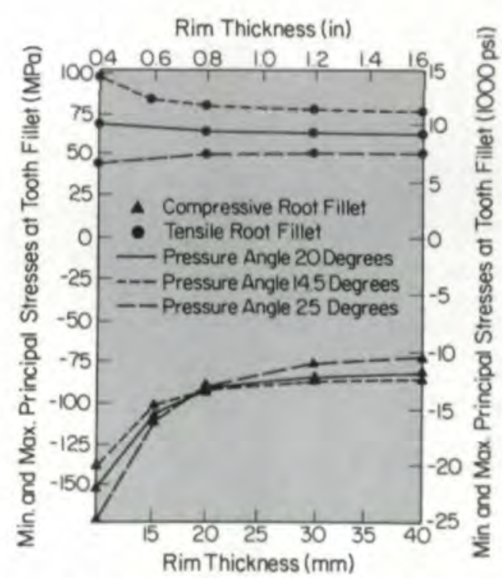

Fig. 25 – Root fillet principal stresses of internal gears with different pressure angles.

answers. There is a relatively new approach to this problem. This approach is called the Boundary Integral Method, which is based on two dimensional theory of elasticity and appropriate transform functions. The solution is exact for the boundary curve chosen and as close as possible to the given one which represents the shape of the stressed piece. Several researchers[8,9] have done investigations on external spur gears, but no research has been done on the internal spur gears. It is believed that the application of this method to the internal gear stress problems can yield satisfactory results, especially in the investigation of the stress concentration around the root fillets. This method is more efficient as far as the CPU time is concerned, and the stress values have better accuracy.

Optimization of Internal Gear Design. The traditional approach to gear design is to utilize design formulas and gear ratings found in standards and codes in order to meet the requirements of the expected operating conditions. This approach does give a feasible solution for a given design; however, it does not guarantee this design is the best possible solution. Nowadays, it is possible to take advantage of high speed digital computers to determine the optimal solution from among many feasible answers. Optimization of the tooth profile geometry is an important area within this field.[10] It is possible to synthesize a noninvolute spur gear pair with optimal load carrying ability based on the bending and contact strength. All these tooth profiles can be synthesized by using man-computer interactive design procedures on CAD/CAM systems.

Summarizing the results and discussion presented here, the following conclusions have been reached:

1. Rim thickness has a dramatic effect on the fillet stresses and stress distribution. When the thickness is less than 4/P, the stress at the tensile fillet changes, and the stress at the compressive fillet increases sharply.
2. As the rim thickness decreases, the position of the maximum stress will tend to move to the bottom of the tooth space apart from the loaded tooth.
3. Rim thickness has a global effect on the stress distribution of the whole gear, and it is recommended that the thickness should be at least 4/P. If the rim is too thin, rim bending may be a severe problem, and the most critical area may shift to the rim.
4. Root fillet radius has a local effect only, and, in order to accurately determine its influences, different element types and meshes should be used. Experimental methods are also suggested.
5. The root fillet should be carefully modelled in order to derive accurate results. Element density and the aspect ratio of elements should be chosen based upon comprehensive study. Experimental data must be used to justify the validity of the models.
6. The fillet stresses vary linearly as the loading position changes, but for thin rim cases, nonlinear relationships are present due to the influence of the deformation of the flexible rim. Usually, if rim thickness is less than 3/P, the rim bending effect will appear.
7. When the loading position approaches the tooth root, the loca-

(continued on page 48)

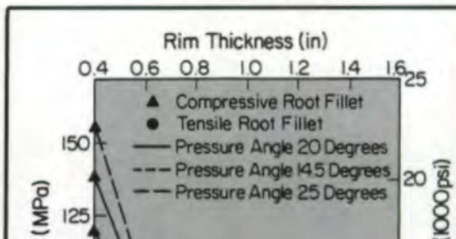

Fig. 26 – Root fillet Von Mises stresses of internal gears with different pressure angles.

BACK TO BASICS...

Helical Gear Mathematics Formulas and Examples

Earle Buckingham
Eliot K. Buckingham
Buckingham Associates, Inc.
Springfield, VT

The following excerpt is from the *Revised Manual of Gear Design, Section III,* covering helical and spiral gears. This section on helical gear mathematics shows the detailed solutions to many general helical gearing problems. In each case, a definite example has been worked out to illustrate the solution. All equations are arranged in their most effective form for use on a computer or calculating machine.

AUTHOR:

ELIOT K. BUCKINGHAM *is president of Buckingham Associates, Inc., a consulting firm working in the areas of design, application and manufacture of gears for any type of drive. Mr. Buckingham earned his B.S. from Massachusetts Institute of Technology and his M.S. from the University of New Mexico. He is the author of* Tables for Recess Action Gears *and numerous technical papers, as well as the revised edition of* The Manual of Gear Design *by Earle Buckingham. He is a member of ASME and a Registered Professional Engineer in the State of Vermont.*

Given the pitch radius and lead of a helical gear, to determine the helix angle:

When,
R = Pitch Radius of Gear
L = Lead of Tooth
ψ = Helix Angle

Then,

$$\text{TAN}\ \psi = \frac{2\pi R}{L}$$

Example: $R = 3.000 \qquad L = 21.000$

$$\text{TAN}\ \psi = \frac{2 \times 3.1416 \times 3.000}{21.000} = .89760 \qquad \psi = 41.911^\circ$$

The involute of a circle is the curve that is described by the end of a line which is unwound from *the circumference of a circle as shown in Fig. 1.*

When,
R_b = Base Radius
θ = Vectorial Angle
r = Length of Radius Vector

Then,

$$\theta = \frac{\sqrt{r^2 - R_b^2}}{R_b} - \text{ARC TAN}\ \frac{\sqrt{r^2 - R_b^2}}{R_b}$$

Given the arc tooth thickness and pressure angle in the plane of rotation of a helical gear at a given radius, to determine its tooth thickness at any other radius:

When,

r_1 = Given Radius

ϕ_1 = Pressure Angle at r_1

T_1 = ARC Tooth Thickness at r_1

r_2 = Radius Where Tooth Thickness Is To Be Determined

ϕ_2 = Pressure Angle at r_2

T_2 = ARC Tooth Thickness at r_2

Then,

$$\text{COS}\ \phi_2 = \frac{r_1\ \text{COS}\ \phi_1}{r_2}$$

$$T_2 = 2\ r_2\left(\frac{T_1}{2r_1} + \text{INV}\ \phi_1 - \text{INV}\ \phi_2\right)$$

Example: $r_1 = 2.500$ $T_1 = .2618$ $r_2 = 2.600$

$\phi_1 = 14.500°$ $\text{COS}\ \phi_1 = .96815$ $\text{INV}\ \phi_1 = .00554$

$$\text{COS}\ \phi_2 = \frac{2.500 \times .96815}{2.600} = .93091$$

$\phi_2 = 21.425°$ $\text{INV}\ \phi_2 = .01845$

$$T_2 = 2 \times 2.600\left(\frac{.2618}{5.000} + .00554 - .01845\right) = .2051$$

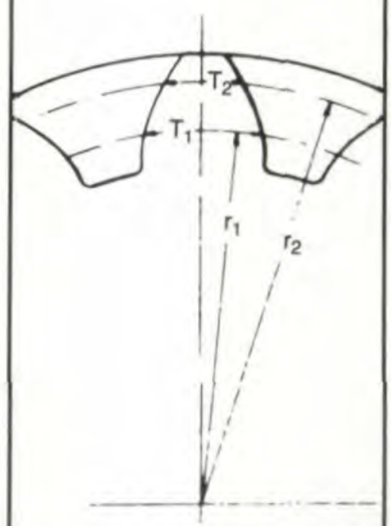

Fig. 2

Given the helix angle, normal diametral pitch and numbers of teeth, to determine the center distance:

When,

ψ = Helix Angle

N_1 = Number of Teeth in Pinion

N_2 = Number of Teeth in Gear

C = Center Distance

P_n = Normal Diametral Pitch

Then,

$$C = \frac{N_1 + N_2}{2\ P_n\ \text{COS}\ \psi}$$

Example: $\psi = 30°$ $P_n = 8$ $N_1 = 24$ $N_2 = 48$ $\text{COS}\ \psi = .86603$

$$C = \frac{24 + 48}{2 \times 8 \times .86603} = 5.1961$$

Given the arc tooth thickness in the plane of rotation at a given radius, to find the normal chordal thickness and the normal chordal addendum:

When, T = ARC Tooth Thickness at R in Plane of Rotation

T_n = Normal Chordal Thickness at R

Q_n = Normal Chordal Addendum

R_o = Outside Radius

R = Pitch Radius

ψ = Helix Angle at R

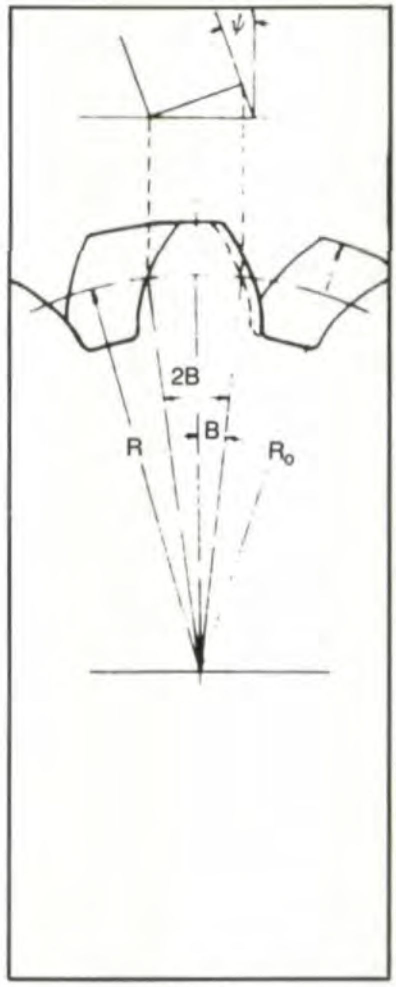

Fig. 3

Then,

$$\text{ARC } B = \frac{T \cos^2 \psi}{2R}$$

$$T_n = \frac{2R \sin B}{\cos \psi}$$

$$Q_n = R_o - \cos B$$

Example: $T = .2267$ $R_o = 1.8570$ $R = 1.7320$

$\psi = 30°$ $\cos \psi = .86603$ $\cos^2 \psi = .75000$

$$\text{ARC } B = \frac{.2267 \times .7500}{2 \times 1.7320} = .04908 \qquad B = 2.812°$$

$\sin B = .04906$ $\cos B = .99880$

$$T_n = \frac{2 \times 1.7320 \times .04906}{.86603} = .1962$$

$$Q_n = 1.8570 - (1.7320 \times .99880) = .1271$$

Given the circular pitch and pressure angle in the plane of rotation and the helix angle of a helical gear, to determine the normal circular pitch and the normal pressure angle:

When, ψ = Helix Angle

ϕ = Pressure Angle in Plane of Rotation

p = Circular Pitch in Plane of Rotation

ϕ_n = Normal Pressure Angle

p_n = Normal Circular Pitch

Then,

$$p = p \cos \psi \qquad \tan \phi_n = \tan \phi \cos \psi$$

Example: $p = .3927$ $\psi = 23°$ $\phi = 20°$ $\cos \psi = .92050$ $\tan \phi = .36397$

$p_n = .3927 \times .92050 = .36148$ $\tan \phi_n = .36397 \times .92050 = .33503$

$\phi_n = 18.522°$

Given the arc tooth thickness and pressure angle in the plane of rotation at a given radius, to determine the radius where the tooth becomes pointed:

When, r_1 = Given Radius

r_2 = Radius where Tooth Becomes Pointed

T_1 = ARC Tooth Thickness at r_1

ϕ_1 = Pressure Angle at r_1

ϕ_2 = Pressure Angle at r_2

Then,

$$\text{INV } \phi_2 = \frac{T_1}{2\, r_1} + \text{INV } \phi_1$$

$$r_2 = \frac{r_1 \text{ COS } \phi_1}{\text{COS } \phi_2}$$

Example: $r_1 = 2.500$ $T_1 = .2618$ $\phi_1 = 14.500°$

$\text{INV } \phi_1 = .00554$

$$\text{INV } \phi_2 = \frac{.2618}{2 \times 2.500} + .00554 = .05790 \text{ Radians}$$

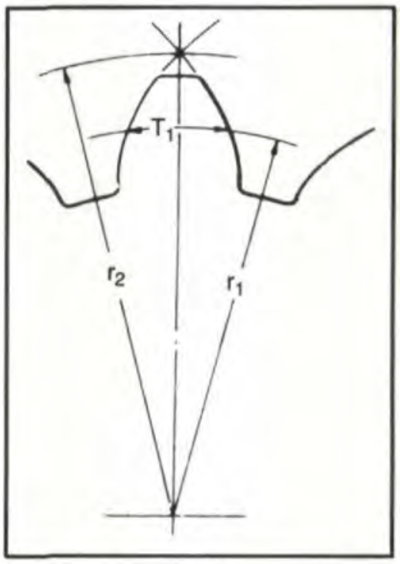

Fig. 4

$\phi_2 = 30.693°$ $\text{COS } \phi_2 = .85991$ $\text{COS } \phi_1 = .96815$

$$r_2 = \frac{2.500 \times .96815}{.85991} = 2.8147$$

Given the normal circular pitch, the normal pressure angle and the helix angle of a helical gear, to determine the circular pitch and the pressure angle in the plane of rotation:

When, ψ = Helix Angle

ϕ_n = Normal Pressure Angle

p_n = Normal Circular Pitch

ϕ = Pressure Angle in Plane of Rotation

p = Circular Pitch in Plane of Rotation

Then,

$$p = \frac{p_n}{\text{COS } \psi} \qquad \text{TAN } \phi = \frac{\text{TAN } \phi_n}{\text{COS } \psi}$$

Example: $\psi = 25°$ $\phi_n = 20°$ $\text{COS } \psi = .90631$ $\text{TAN } \phi_n = .36397$ $p_n = .5236$

$$p = \frac{.5236}{.90631} = .57772 \qquad \text{TAN } \phi = \frac{.36397}{.90631} = .40159 \qquad \phi = 21.880°$$

Given the tooth proportions in the plane of rotation of a pair of helical gears (parallel shafts), to determine the center distance at which they will mesh tightly:

When,

r_1 = Given Radius of 1st Gear

r_2 = Given Radius of 2nd Gear

N_1 = Number of Teeth in 1st Gear

N_2 = Number of Teeth in 2nd Gear

ϕ_1 = Pressure Angle at r_1 and r_2

ϕ_2 = Pressure Angle at Meshing Position

T_1 = ARC Tooth Thickness at r_1

T_2 = ARC Tooth Thickness at r_2

C_1 = Center Distance for Pressure Angle ϕ_1

C_2 = Center Distance for Pressure Angle ϕ_2

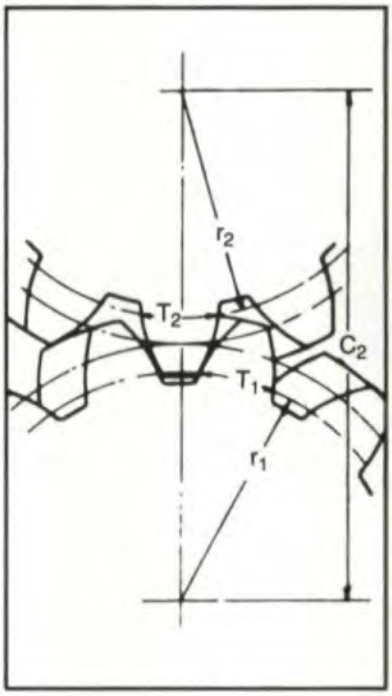

Fig. 5

Then,

$$\text{INV}\ \phi_2 = \frac{N_1 (T_1 + T_2) - 2\pi r_1}{2 r_1 (N_1 + N_2)} + \text{INV}\ \phi_1$$

$$C_1 = r_1 + r_2$$

$$C_2 = \frac{C_1 \cos \phi_1}{\cos \phi_2}$$

Example: $r_1 = 2.500$ $T_1 = .2800$ $N_1 = 30$ $\phi_1 = 14.500°$

$r_2 = 4.000$ $T_2 = .2750$ $N_2 = 48$ $C_1 = 6.500$

$$\text{INV}\ \phi_2 = \frac{30\ (.2800 + .2750) - 2\pi \times 2.500}{2 \times 2.500\ (30 + 48)} + .00545 = .007955$$

$\phi_2 = 16.315°$ $\cos \phi_2 = .95973$

$$C_2 = \frac{6.500 \times .96815}{.95973} = 6.5570$$

Given the pitch radius and helix angle of a helical gear, to determine the lead of the tooth.

When,

R = Pitch Radius

L = Lead of Tooth

ψ = Helix Angle

Then,

$$L = \frac{2\pi R}{\text{TAN}\ \pi}$$

Example: R = 2.500 $\psi = 22.50°$ $\text{TAN}\ \psi = .41421$

$$L = \frac{2 \times 3.1416 \times 2.500}{.41421} = 37.9228$$

Given the number of teeth, helix angle and proportions of the normal basic rack of a helical gear, to determine the pitch radius and the base radius:

When,
N = Number of Teeth
ψ = Helix Angle at R
P_n = Normal Diametral Pitch
R = Pitch Radius
ϕ_n = Normal Pressure Angle
ϕ = Pressure Angle in Plane of Rotation
R_b = Base Radius

Then,

$$R = \frac{N}{2 P_n \cos \psi} \qquad \tan \phi = \frac{\tan \phi_n}{\cos \psi}$$

$$R_b = R \cos \phi = \frac{N \cos \phi}{2 P_n \cos \psi}$$

Example: $N = 30$ $\quad \psi = 25°$ $\quad P_n = 6$ $\quad \phi_n = 14\frac{1}{2}°$ $\quad \cos \psi = .90631$ $\quad \tan \phi_n = .25862$

$$R = \frac{30}{2 \times 6 \times .90631} = 2.7584$$

$$\tan \phi = \frac{.25862}{.90631} = .28535 \qquad \phi = 15.926° \qquad \cos \phi = .96162$$

$$R_b = \frac{30 \times .96162}{2 \times 6 \times .90631} = 2.65256$$

Given the normal diametral pitch, numbers of teeth and center distance, to determine the lead and helix angle:

When,
N_1 = Number of Teeth in Pinion
N_2 = Number of Teeth in Gear
P_n = Normal Diametral Pitch
C = Center Distance
ψ = Helix Angle
L_1 = Lead of Pinion
L_2 = Lead of Gear

Then,

$$\cos \psi = \frac{N_1 + N_2}{2 P_n C} \qquad L_1 = \frac{\pi N_1}{P_n \sin \psi} \qquad L_2 = \frac{\pi N_2}{P_n \sin \psi}$$

Example: $P_n = 6$ $\quad N_1 = 18$ $\quad N_2 = 30$ $\quad C = 4.500$

$$\cos \psi = \frac{18 + 30}{2 \times 6 \times 4.500} = .88889 \qquad \psi = 27.266° \qquad \sin \psi = .45812$$

$$L_1 = \frac{3.1416 \times 18}{6 \times .45812} = 20.5728 \qquad L_2 = \frac{3.1416 \times 30}{6 \times .45812} = 34.2880$$

Given the tooth proportions in the plane of rotation of a helical gear, to determine the position of a mating rack of different circular pitch and pressure angle:

When, ψ_1 = Given Helix Angle at R_1

ψ_2 = Helix Angle for Mating Rack

ψ_b = Base Helix Angle

ϕ_{n1} = Normal Pressure Angle at R_1

ϕ_{n2} = Pressure Angle of Mating Rack

ϕ_1 = Pressure Angle at R_1 in Plane of Rotation

ϕ_2 = Pressure Angle of Mating Rack in Plane of Rotation

R_1 = Given Pitch Radius

R_2 = Pitch Radius with Mating Rack

R_b = Base Radius

a = Addendum of Rack

T_1 = ARC Tooth Thickness at R_1

N = Number of Teeth

X = Distance from Center of Gear to Tip of Rack Tooth

p_{n1} = Normal Circular Pitch at R_1

p_{n2} = Normal Circular Pitch of Rack

Note: (p_{n1} COS ϕ_{n1} Must Be Equal To (p_{n2} COS ϕ_{n2})

Then,

$$\text{SIN } \psi_b = \text{SIN } \psi_1 \text{ COS } \phi_{n1}$$

$$\text{SIN } \psi_2 = \frac{\text{SIN } \psi_b}{\text{COS } \phi_{n2}} = \frac{\text{SIN } \psi_1 \text{ COS } \phi_{n1}}{\text{COS } \phi_{n2}}$$

$$\text{TAN } \phi_2 = \frac{\text{TAN } \phi_{n2}}{\text{COS } \psi_2} \qquad R_2 = \frac{R_b}{\text{COS } \phi_2}$$

$$X = R_2 - a + \frac{1}{2 \text{ TAN } \phi_2}\left[2 R_2\left(\frac{T_1}{2 R_1} + \text{INV } \phi_1 - \text{INV } \phi_2\right) - \frac{\pi R_2}{N}\right]$$

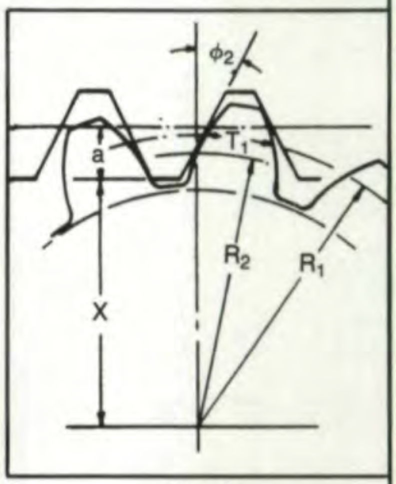

Fig. 6

Example: $\psi_1 = 25°$ $\quad \phi_{n1} = 14½°$ $\quad \phi_1 = 15.926°$ $\quad R_1 = 2.7584$ $\quad R_b = 2.65256$

$\phi_{n2} = 20°$ $\quad a = .185$ $\quad T_1 = .2888$ $\quad N = 30$

SIN ψ_1 = .42262 $\quad$ COS ψ_1 = .90631 $\quad$ TAN ϕ_{n1} = .25862 $\quad$ TAN ϕ_{n2} = .36397

p_{n1} = .5236 $\quad$ p_{n2} = .53946 $\quad$ COS ϕ_{n1} = .96815 $\quad$ COS ϕ_{n2} = .93969

[p_{n1} COS ϕ_{n1} = .50692] = [p_{n2} COS ϕ_{n2} = .50692]

$$\text{SIN } \psi_2 = \frac{.42262 \times .96815}{.93969} = .43542 \qquad \psi_2 = 25.812° \qquad \text{COS } \psi_2 = .90023$$

$$\text{TAN } \phi_2 = \frac{.36397}{.90023} = .40431 \qquad \phi_2 = 22.014° \qquad \text{COS } \phi_2 = .92709$$

INV ϕ_2 = .020093 $\quad$ INV ϕ_1 = .007387

$$R_2 = \frac{2.65256}{.92709} = 2.86117$$

$$X = 2.86117 - .185 + \frac{1}{2 \times .40431}\left[5.72234\left(\frac{.2888}{5.5168} + .007387 - .020093\right) - \frac{.31416 \times 2.86117}{30}\right] = 2.5729$$

Given the center distance, number of teeth and basic rack proportions (hob proportions) of a pair of helical gears, to determine the hobbing data:

When,

ϕ_{nc} = Pressure Angle of Hob
p_{nc} = Diametral Pitch of Hob
a_c = Addendum of Hob
C_1 = Center Distance with Pressure Angle of ϕ_1
C_2 = Given Center Distance of Operation
N_1 = Number of Teeth in Pinion
R_{o1} = Outside Radius of Pinion
R_{r1} = Root Radius of Pinion
L_1 = Lead of Pinion
R_1 = Pitch Radius of Pinion
b_1 = Dedendum of Pinion
ψ_1 = Helix Angle of Generation
N_2 = Number of Teeth in Gear
R_{o2} = Outside Radius of Gear
R_{r2} = Root Radius of Gear
L_2 = Lead of Gear
R_2 = Pitch Radius of Gear
b_2 = Dedendum of Gear
ψ_2 = Helix Angle of Operation
ϕ_1 = Pressure Angle of Generation in Plane of Rotation
ϕ_2 = Pressure Angle of Operation in Plane of Rotation
p_1 = Diametral Pitch of Generation in Plane of Rotation
h_t = Total Tooth Depth of Gears

Then, Make trial calculation for lead as follows:

$$\text{COS}\ \psi_1 = \frac{N_1 + N_2}{2\, p_{nc}\, C_2}$$

$$L_1 = \frac{\pi N_1}{p_{nc}\ \text{SIN}\ \psi_1} \qquad L_2 = \frac{\pi N_2}{p_{nc}\ \text{SIN}\ \psi_1}$$

Select values for L_1 and L_2 which can be readily obtained on the hobbing machine:

Then,

$$\text{SIN}\ \psi_1 = \frac{\pi N_1}{p_{nc} L_1} = \frac{\pi N_2}{p_{nc} L_2} \qquad \text{TAN}\ \phi_1 = \frac{\text{TAN}\ \phi_{nc}}{\text{COS}\ \psi_1}$$

$$p_1 = p_{nc}\ \text{COS}\ \psi_1 \qquad C_1 = \frac{N_1 + N_2}{2\, p_1} \qquad \text{COS}\ \phi_2 = \frac{C_1\ \text{COS}\ \phi_1}{C_2}$$

$$(R_{r1} + R_{r2}) = C_1 - 2\, a_c + \frac{C_1}{\text{TAN}\ \phi_1}(\text{INV}\ \phi_2 - \text{INV}\ \phi_1)$$

$$b_1 = \frac{C_2 - (R_{r1} + R_{r2})}{1 + \sqrt{\frac{N_2}{N_1}}} \qquad b_2 = \frac{C_2 - (R_{r1} + R_{r2})}{1 + \sqrt{\frac{N_1}{N_2}}}$$

Note: When smallest N is 30 or more, then, $b_1 = b_2 = \frac{C_2 - (R_{r1} + R_{r2})}{2}$

$$R_1 = \frac{N_1 C_2}{N_1 + N_2} \qquad R_2 = \frac{N_2 C_2}{N_1 + N_2} \qquad R_{r1} = R_1 - b_1 \qquad R_{r2} = R_2 - b_2$$

$$h_t = .932\, [C_2 - (R_{r1} + R_{r2})\,] \qquad R_{o1} = R_{r1} + h_t \qquad R_{o2} = R_{r2} + h_t$$

$$\text{TAN}\ \psi_2 = \frac{2\,\pi R_1}{L_1} = \frac{2\,\pi R_2}{L_2}$$

(Continued on next page)

Example: $N_1 = 20$ $N_2 = 60$ $p_{nc} = 5$ $A_c = .2314$ $C_2 = 9.00$

$\phi_{nc} = 14.500$ $\text{TAN}\ \phi_{nc} = .25862$

Trial Calculation:

$$\text{COS}\ \psi_1 = \frac{20 + 60}{2 \times 5 \times 9.00} = .88889 \qquad \psi_1 = 27.266° \qquad \text{SIN}\ \psi = .45812$$

$$L_1 = \frac{20\ \pi}{5 \times .45812} = 27.4303 \qquad L_2 = \frac{60\ \pi}{5 \times .45812} = 82.2909$$

We will select the following values for L_1 and L_2:

$$L_1 = 27.500 \qquad L_2 = 82.500$$

$$\text{SIN}\ \psi = \frac{20\ \pi}{5 \times 27.500} = .45696 \qquad \psi_1 = 27.1910 \qquad \text{COS}\ \psi_1 = .88949$$

$$\text{TAN}\ \phi_1 = \frac{.25862}{.88969} = .29069 \qquad \phi_1 = 16.208° \qquad \text{COS}\ \phi_1 = .96025 \qquad \text{INV}\ \phi_1 = .007796$$

$$p_1 = 5 \times .88949 = 4.44745 \qquad C_1 = \frac{20 + 60}{2 \times 4.44745} = 8.99392$$

$$\text{COS}\ \phi_2 = \frac{8.99392 \times .96025}{9} = .95960 \qquad \phi_2 = 16.3416 \qquad \text{INV}\ \phi_2 = .007994$$

$$(R_{r1} + R_{r2}) = 8.99392 - 2 \times .2314 + \frac{8.99392}{.29069} [.007994 - .007796] = 8.5372$$

$$b_1 = \frac{9.00 - 8.5372}{1 + \sqrt{60/20}} = .16938 \qquad b_2 = \frac{9.00 - 8.5372}{1 + \sqrt{20/60}} = .29340$$

$$R_1 = \frac{20 \times 9.00}{20 + 60} = 2.250 \qquad R_2 = \frac{60 \times 9.00}{20 + 60} = 6.750$$

$$R_{r1} = 2.250 - .16938 = 2.08062 \qquad R_{r2} = 6.750 - .29340 = 6.45660$$

$$h_t = .932\ [9.00 - 8.5372] = .43133$$

$$R_{o1} = 2.08062 + .43133 = 2.51195 \qquad R_{o2} = 6.45660 + .43133 = 6.88793$$

$$\text{TAN}\ \psi_2 = \frac{2\ \pi\ 2.250}{27.5} = .514079 \qquad \psi_2 = 27.207$$

The specifications for this pair of gears are as follows:

$N_1 = 20$	$R_{r1} = 2.08062$	$L_2 = 82.500$	Helix angle for hobbing = 27.1910
$R_{o1} = 2.51195$	$N_2 = 60$	$R_{r2} = 6.45660$	
$R_1 = 2.250$	$R_{o2} = 6.88793$	$C_2 = 9.00$	
$L_1 = 27.500$	$R_2 = 6.750$		

Given the proportions of an internal helical gear drive, to determine the contact ratio:

When,
R_1 = Pitch Radius of Helical Gear
R_{o1} = Outside Radius of Helical Gear
R_{b1} = Base Radius of Helical Gear
ϕ = Pressure Angle in Plane of Rotation
p = Circular Pitch in Plane of Rotation
C = Center Distance
m_p = Contact Ratio
R_2 = Pitch Radius of Internal Gear
R_i = Internal Radius of Internal Gear
R_{b2} = Base Radius of Internal Gear

Then,

$$m_p = \frac{\sqrt{R_{o1}{}^2 - R_{b1}{}^2} + C \text{ SIN } \phi - \sqrt{R_i^2 - R_b{}^2}}{p \text{ COS } \phi}$$

Example: $R_1 = 1.250$ $R_{o1} = 1.4375$ $R_{b1} = 1.1746$ $\phi = 20°$ $p = .3927$

$R_2 = 3.500$ $R_i = 3.4375$ $R_{b2} = 3.2888$ $C = 2.250$

SIN ϕ = .34202 COS ϕ = .93969

$$m_p = \frac{\sqrt{(1.4375)^2 - (1.1746)^2} + (2.250 \times .34202) - \sqrt{(3.4375)^2 - (3.2888)^2}}{.3927 \times .93969} = 1.62$$

Given the proportions of a pair of helical gears (external or internal), to determine the face contact ratio:

When,
F = Face Width
p = Circular Pitch in Plane of Rotation
ψ = Helix Angle
m_f = Face Contact Ratio

Then,

$$m_f = \frac{F \text{ TAN } \psi}{p}$$

Example: $F = 1.500$ $p = .3927$ $\psi = 30°$ TAN ψ = .57735

$$m_f = \frac{1.500 \times .57735}{.3927} = 2.20$$

Given the proportions of a pair of helical gears (external or internal), to determine the total contact ratio:

When,
m_p = Contact Ratio
m_f = Face Contact Ratio
m_t = Total Contact Ratio

Then,

$$m_t = m_p + m_f$$

Example: $m_p = 1.59$ $m_f = 2.20$

$m_t = 1.59 + 2.20 = 3.79$

TOOTH ROOT STRESSES . . .
(continued from page 20)

estimated), the amount of crowning should be chosen in such a way that when applying the service load, the lowest root stresses will be the result. This criterion is satisfied when the *product*

$$K_c = K_{F\beta-c} \cdot Y_\gamma \cdot K_{F\beta-f}$$

reaches a minimum.

As an example this optimization is performed for the test gears in Fig. 18. One can see that the curve for K_c has a flat minimum in the area of small crowning values (near gear set B). This result seems to be plausible because of the very stiff test rig.

It should be noted that the optimization method introduced here is only based on the tooth root stresses and should only be used if tooth breakage is the critical failure criterion. An optimization for contact stresses may be quite different and usually provides a guide to higher amounts of crowning.

Summary

By strain gauge measurements of spiral bevel gears, the influence of lengthwise crowning and relative displacements between pinion and gear on tooth root stresses was investigated. It was found that the crowning effects the load distribution over the lines of contact and the load sharing between pairs of teeth meshing simultaneously. For both influences a quantitative description could be derived.

(continued on page 47)

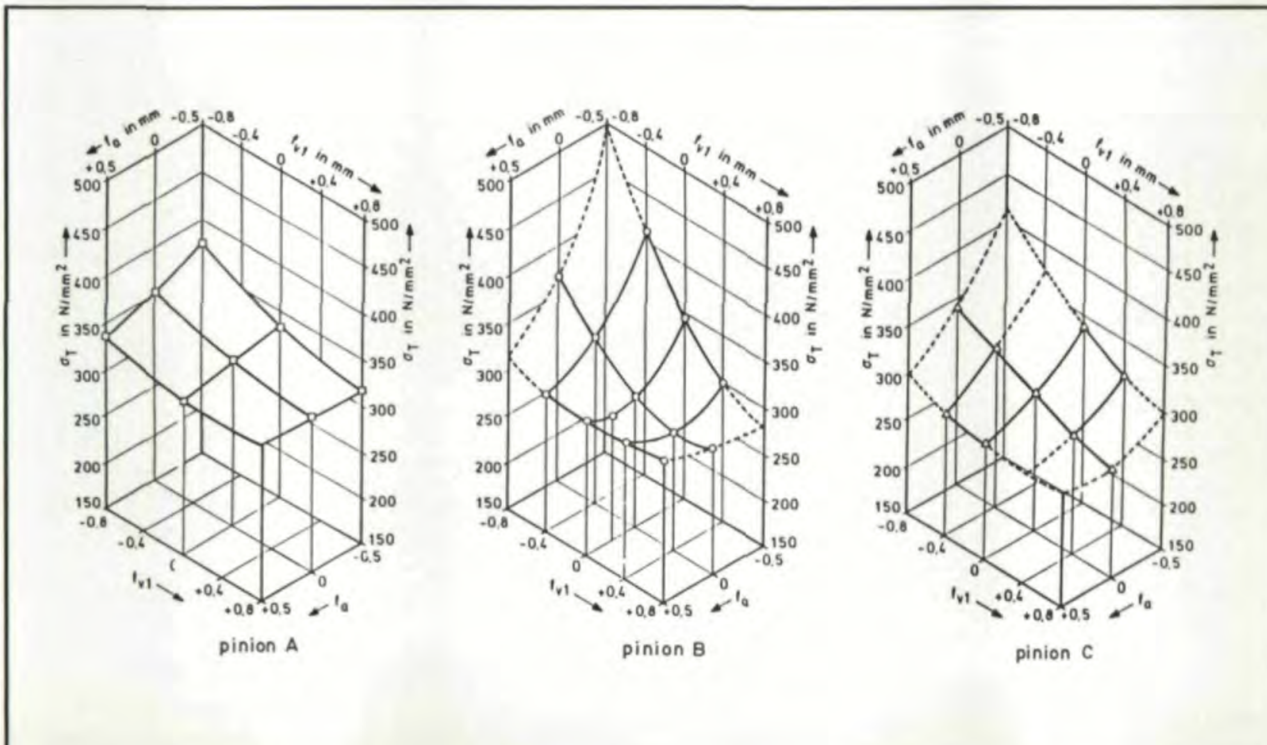

Fig. 16 – Influence of combined displacements on the maximum root stresses $\sigma_{T\ max}$ at the pinions. (Amount of crowning, see Fig. 2.)

CLASSIFIED

Rates: Classified Display—per inch (minimum 3") **1X**-$120, **3X**-$110, **6X**-$100. Type will be set to advertiser's layout or *Gear Technology* will set type at no extra charge. **Word Count:** 35 characters per line, 7 lines per inch.

Payment: Full payment must accompany classified ads. Mail copy to *Gear Technology,* P.O. Box 1426, Elk Grove Village, IL 60007. **Agency Commission:** No agency commision on classifieds.

Materials Deadline: Ads must be received by the 25th of the month, two months prior to publication. **Acceptance:** Publisher reserves the right to accept or reject classified advertisements at his discretion.

COMPUTER AIDS

GEAR ESTIMATING

The COSTIMATOR® computer aided cost estimating system insures speed and consistency in the difficult task of estimating the costs of all types of gears.

Used by small shops and Fortune 500 companies throughout the country.

For complete information contact us today.

Manufacturers Technologies, Inc.
59G Interstate Dr.
West Springfield, MA 01089
(413) 733-1972

CIRCLE A-16 ON READER REPLY CARD

GEAR CALCULATION PROGRAMS FOR THE GEAR MANUFACTURER

INEXPENSIVE, EASY TO RUN ON IBM COMPATIBLES

EXTERNAL — INCH (DP)
INTERNAL — METRIC (Mod.)
SPUR
HELICAL

STRAIGHT BEVEL (104)
SPIRAL BEVEL #16 & 27 GRD
BLANK AND SUMMARIES

For Brochure and More Information
CALL OR WRITE
UNIVERSAL GEAR CO. INC.
P.O.Box A.G., Anza, CA 92306
(714) 763-4616

CIRCLE A-17 ON READER REPLY CARD

GEARTECH Software, Inc.

GEAR DESIGN/ANALYSIS for IBM PC & compatibles. GEARCALC ($995): design optimum spur & helical gearsets from application data. AGMA218 ($1495): calculate pitting and bending fatigue lives per AGMA Std. 218.01. SCORING+ ($495): analyze/plot scoring & wear probabilities. Fast, menu-driven programs work as one system (combined price $2495), do extensive error-checking. Comprehensive manuals (theory, operation, examples) included. Demo available. GEARTECH Software, Inc., 1017 Pomona Ave., Albany, CA 94706 (415) 524-0668.

CIRCLE A-18 ON READER REPLY CARD

COMPUTER AIDS

GEARS-SPLINES

DESIGN AND TOOLING

- Custom gear design including non-standard pressure angles for more strength.
- Programs to enter tooling data into computer files and search for existing cutters to cut a new gear or spline.
- Gearing computer software for sale.
- Consulting services for gear and spline problems.

VAN GERPEN-REECE ENGINEERING
1502 Grand Blvd.
Cedar Falls, Iowa 50613
(319) 266 4674

CIRCLE A-27 ON READER REPLY CARD

REBUILDING

HOBBER REBUILDING SPECIALISTS

Having trouble meeting today's demand quality control tolerances? Let our factory trained and experienced staff return your machine to optimum operating condition.

We specialize in repairing, rebuilding and modernizing all makes of hobbers.

- Cleveland Rigidhobbers
- Gould & Eberhardt
- Barber Colman

PRESSMATION INC.
522 Cottage Grove Road
Bloomfield, Conn. 06002
(203) 242-8525

CIRCLE A-25 ON READER REPLY CARD

SUBCONTRACT

GEAR TOOTH GRINDING & HONING ONLY

Production Quantities
3/4" P.D. to 27.5" P.D.;
3.5 D.P. and 11" Face

Gear Tooth Finishing is our Only Business

We have no turning, hobbing or shaping capability

ALLEGHENY GEAR CORP.
23 Dick Road
Depew, NY 14043
716-684-3811

MEMBER OF AGMA

CIRCLE A-23 ON READER REPLY CARD

Bring in new customers for your business by advertising in GEAR TECHNOLOGY, The Journal of Gear Manufacturing.
Call (312) 437-6604

There's still time . . .
order closing date for a classified ad in the July/August issue is May 10th.

TOOTH ROOT STRESSES . . .

(continued from page 45)

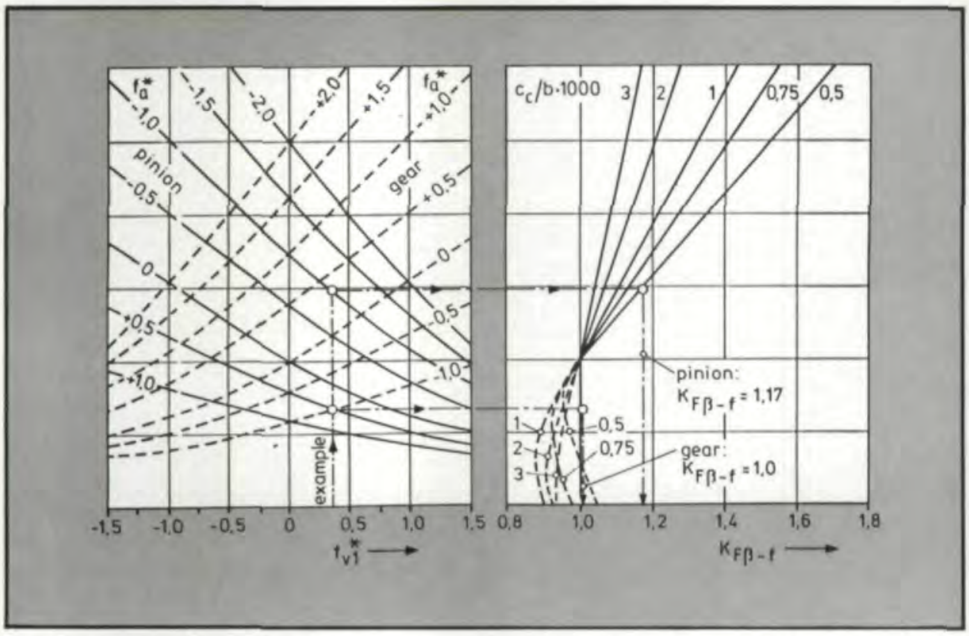

Fig. 17—Nomogram for determining the displacement factor $K_{F\beta-f}$ ($f_{v1}^* = f_{v1}/d_{m2} \cdot 1000$, $f_a^* = f_a/d_{m2} \cdot 1000$).

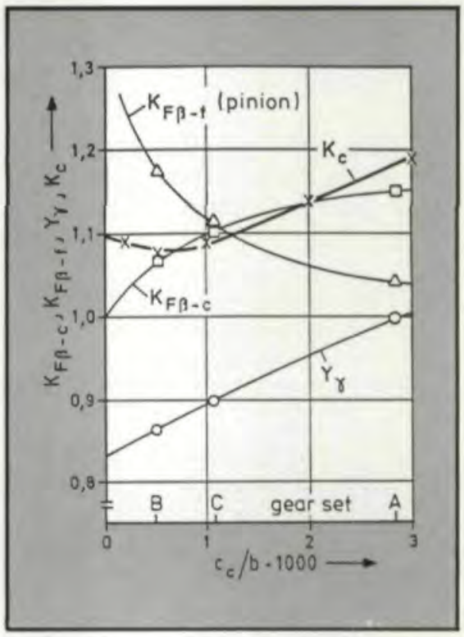

Fig. 18—Optimization of lengthwise crowning.

In the case of relative displacements, deviations in pinion mounting distance and in offset have the strongest influence on the root stresses. A method was introduced to determine the increase or decrease of maximum stresses that have to be expected for a combination of certain values of these parameters. Further, a optimization criterion was derived that allows finding the amount of lengthwise crowning producing the lowest root stresses for a certain service condition.

References

1. WINTER, H., PAUL, M. "Influence of Relative Displacements Between Pinion and Gear on Tooth Root Stresses of Spiral Bevel Gears." *Gear Technology*, July/August, 1985.
2. JARAMILLO, T.J. "Deflections and Moments due to a Concentrated Load on a Cantilever Plate of Infinite Length." *Journal of Applied Mechanics*, Vol. 17, Trans., ASME, Vol. 72 1950, S. 67-72, 342-343.
3. WELLAUER, E.J., SEIREG, A. "Bending Strength of Gear Teeth by Cantilever Plate Theory." *Journal of Engineering for Industry*. Trans. ASME, Aug. 1960, S. 213-222.
4. *AGMA 2003 – A86: Standard for Rating the Pitting Resistance* and Bending Strength of Generated Straight Bevel, Zerol Bevel and Spiral Bevel Gear Teeth. 1986.
5. DIN 3991: Tragfähigkeitsberechnung von Kegelrädern ohne Achsversetzung; Normentwurf. 1986.
6. COLEMAN, W. "Improved Method for Estimating Fatigue Life of Bevel and Hypoid Gears." *SAE Quarterly Transactions*. Vol. 6, No. 2, 1952.
7. COLEMAN, W. "Effect of Mounting Displacements on Bevel and Hypoid Gear Tooth Strength." SAE-Paper 75 01 51. 1975.

TECHNICAL CALENDAR

JUNE 22-24. University of Wisconsin-Milwaukee, Microcomputer Applications in Worm Gear Design & Analysis. A workshop enabling students to develop customized computer-aided gear design systems. For further information, contact: John M. Leaman, Center for Continuing Engineering Education, UW-M, 929 N. 6th St., Milwaukee, WI 53203. (414) 227-3110.

AUGUST 10-12. Ohio State University, Gear Noise Course. Material covered includes noise measurement and analysis, causes, reduction techniques, modeling and modal analysis of gear boxes. For further information, contact: Mr. Richard D. Frasher, College of Engineering, OSU, 2070 Neil Ave., Columbus, OH 43210. (614) 292-8143.

SEPTEMBER 27-29. American Society for Metals 11th Annual Heat Treating Conference, McCormick Place, Chicago, IL. Presentations on subjects including heat treating, statistical process control, new energy applications, quenching and cooling improvements. For further information, contact: ASM International, Metals Park, OH 44073. (216) 338-5151.

NOVEMBER 5-10. International Conference on Gearing, Zhengzhou, China. ASME-GRI and several international gear organizations are sponsoring this meeting. For more information contact: Inter—Gear '88 Secretariat, Zhengzhou Research Institute of Mechanical Engineering, Zhongyuan Rd, Zhengzhou, Henan, China. Tel: 47102. Cable 3000. Telex 46033 HSTEC CN.

NOVEMBER 8-10. American Society for Metals Near Net Shape Manufacturing Conference, Hyatt Regency, Columbus, OH. Program will cover precision casting, powder metallurgy, design of dies and molds, forging technology and inspection of precision parts. For further information contact: Technical Department Marketing, ASM International, Metals Park, OH 44073.

CALL FOR PAPERS—The Society of anufacturing Engineers for its **1988 Gear Processing & Manufacturing Clinic, Nov. 15-17, Indianapolis, IN.** Some suggested topics include gear basics, shaper cutter applications, automotive applications, aerospace gears, heat treating and workholding devices. For further information, contact: Joseph A. Franchini, SME, One SME Drive, P.O. Box 930, Dearborn, MI 48121. (313) 271-1500 x394.

CALL FOR PAPERS — Tennessee Technological University for its **1st Internat'l Applied Mechanical Systems Design Conference, March 19-22, 1989, Nashville, TN.** Papers are invited on general mechanical systems subjects including strength, fatigue life, kinematics, vibration, robotics, CAD/CAM, and tribology. Deadline for first drafts is Oct. 1, 1988. For further information, contact: Dr. Cemil Bagci, Dept. of Mech. Eng., TTU, Cookeville, TN 38505. (615) 372-3265.

COMPUTER-AIDED DESIGN . . .
(continued from page 34)

tion of the maximum stress will tend to move to the bottom of the tooth space apart from the loaded tooth.

8. Support conditions do not change the stress distribution or fillet stresses very much for a rigid rim. For thin rim gears, support conditions become an important issue. It may affect the rigidity of the rim and thus increase the stresses considerably.
9. For a rigid rim, the larger the pressure angle, the smaller the root fillet stress. But for thin rims, the larger the pressure angle, the larger the fillet stress.
10. Internal spur gears with different pressure angles respond the same way to the influences of rim thickness, support conditions, loading positions, etc.

References

1. DRAGO, RAYMOND J., PIZZIGATI, Gary A. "Some Progress in the Accurate Evaluation of Tooth Root and Fillet Stresses in Lightweight, Thin-Rimmed Gears", AGMA Paper 229.21, Fall Technical Meeting, Washington, D.C., October, 1980.
2. AGMA Publication 225.01.
3. AGMA Gear Rating Coordinating Committees. "Coordinated Rating for the Strength of Gear Teeth", Publication 229.03, June, 1956.
4. AGMA. "AGMA Manual for Machine Tool Gearing", AGMA 360.02, December, 1971.
5. AGMA. "USA Standard Tooth Proportions for Coarse-Pitch Involute Spur Gears", AGMA 201.02, August, 1968.
6. HWANG, JENG-FONG. "Advanced Computer-Aided Design Method on the Stress Analysis of Internal Spur Gears". Masters Thesis, The Ohio State University, 1986.
7. AIDA, TOSHIO, et al. "Bending Stresses of Internal Spur Gear". *Bulletin of JSME*, Volume 25, No. 202, April, 1982.
8. BARONET, C.N. TORDION, G.V. "Exact Stress Distribution in Standard Gear Teeth and Geometry Factors" *Journal for Industry*, ASME Transaction, Volume 95, November, 1973.
9. RUBENCHIK, V. "Boundary Integral Equation Method Applied to Gear Strength Rating". *Transaction of AMSE, Journal of Mechanisms, Transmission and Automation in Design.* Volume 105, March, 1983.
10. SEIREG, ALI, "State-of-the-Art Review of Computer Optimization of Gear Design". *Journal of Mechanical Design*, Transactions of ASME. Volume 103, January, 1981.